



universität
wien

MASTERARBEIT / MASTER'S THESIS

Titel der Masterarbeit / Title of the Master's Thesis

„QCM studies for the detection of *Staphylococcus epidermidis*“

verfasst von / submitted by

Mathias Petsovits BSc

angestrebter akademischer Grad / in partial fulfillment of the requirements for the degree of

Master of Science (MSc)

Wien, 2016 / Vienna 2016

Studienkennzahl lt. Studienblatt /
degree programme code as it appears on
the student record sheet:

A 066 862

Studienrichtung lt. Studienblatt /
degree programme as it appears on
the student record sheet:

Masterstudium Chemie

Betreut von / Supervisor:

Univ.-Prof. Mag. Dr. Peter Lieberzeit

Mitbetreut von / Co-Supervisor:

ACKNOWLEDGEMENTS

I want to thank everyone who was involved in the implementation of this thesis.

My special thanks go to Univ.-Prof. Mag. Dr. Peter Lieberzeit, my supervisor, for the opportunity to carry out the practical as well as the writing part of my master thesis in his friendly and helpful research group and for his support and advice.

I furthermore want to thank the members of his research group for technical and scientific support, many interesting discussions, and for all the help and advice.

In addition I wish to express my gratitude to the students of the AFM lab courses, who did some of the AFM measurements presented in this work.

Last but not least I need to thank my wonderful girlfriend and my family for their moral support throughout my whole study and life in general. I would not be where I am without them.

The research leading to these results has received funding from the European Union's Seventh Framework Programme FP7/2007-2013 under grant agreement n°312330.

ABSTRACT

Staphylococcus epidermidis is a potential pathogen and a skin colonizing bacterium, which may be used as biological weapon in water supply chains by terrorists. The risk of a terrorist attack triggers the need of a cheap, fast and reliable monitoring system, which can most easily be implemented by a chemical sensor.

This work therefore focuses on the development of a chemical sensor using the mass-sensitive quartz crystal microbalance as transducer and a molecularly imprinted polymer (MIP) thin film as the sensitive layer for the detection of *S. epidermidis*.

Firstly, a stability study of the analyte revealed that frozen analyte solutions are stable for at least 7 days. Then polymer screening for natural affinity of the microorganism featuring 5 different polymers, namely polyurethane, polymethacrylic acid, polystyrene, polyvinylpyrrolidone and polyacrylamide, revealed that polyurethane shows the highest inherent affinity for *S. epidermidis*.

Sensor optimization first comprised of layer thickness optimization and polymer composition. Secondly, it also required to assess removal of the bacterium from the polymers. QCMs produced under optimized conditions, namely using catalyzed polyurethane with the same amount of OH and OCN groups, spin coating with 30 μ l polymer solution at a 7:3 dilution and 1500 rpm rotation speed at 5 s spin time, have then been tested for sensitivity and selectivity. They showed no selectivity against *Bacillus cereus* and *Escherichia coli*, as the signal intensities for these organisms were up to 3 times higher than those for the analyte. Therefore the polymer system was changed to polymethacrylic acid, the second best suited one.

For polymethacrylic acid optimization steps included layer thickness and removal studies, as the composition was not varied in this case. Stamps using immobilization with APTES were also tested as imprinting method, without success. Sedimentation imprinted QCMs using 10 μ l 1:4 diluted polymer solution at 3000 rpm rotation speed for 5 s showed good results. Sensors produced under these conditions were tested for their sensor parameters, namely response time, selectivity, reversibility and limit of detection. The estimated limit of detection was 4.5×10^6 cells / ml and the response time 3 min \pm 20 sec. The selectivity was estimated as ratio of the signal intensities of *S. epidermidis* and *B. cereus* solutions, where the target analyte showed responses 70 times higher than those for *B. cereus*.

Furthermore a new response mechanism is presented and prospects for future work on the topic of detecting *S. epidermidis* are briefly discussed.

ZUSAMMENFASSUNG

Staphylococcus epidermidis ist ein potentiell pathogenes, die menschliche Haut bewohnendes Bakterium, welches von Terroristen als biologischer Kampfstoff in Trinkwasserversorgungssystemen eingesetzt werden könnte. Die Gefahr eines Terrorattentates erklärt die Notwendigkeit der konstanten Wasserüberwachung. Diese sollte mit günstig zu produzierenden, schnellen und verlässlichen Systemen erfolgen, was sich am leichtesten mit chemischen Sensoren realisieren lässt. Die vorliegende Arbeit befasst sich mit der Entwicklung eines chemischen Sensors, welcher auf der Quarzmikrowaage (QCM) als Transducer und einem molekular geprägten Polymer (MIP) als sensitiver Schicht beruht.

Zuerst wurde eine Stabilitätsstudie gefrorener *S. epidermidis* Proben durchgeführt, welche zeigte, dass die gefrorenen Lösungen mindestens 7 Tage stabil sind. Ein Polymerscreening mit 5 verschiedenen Polymere, nämlich Polyurethan, Polymethacrylsäure, Polyvinylpyrrolidon, Polystyrol und Polyacrylamid, zeigte, dass Polyurethan die höchste natürliche Affinität zu *S. epidermidis* aufweist.

Optimierungsexperimente für die Sensorproduktion umfassten Schichtdickenbestimmungen, Variation der Polymerzusammensetzung, sowie die Entfernung der geprägten Organismen. Katalysiertes Polyurethan mit gleichen Mengen an OH und OCN Gruppen entpuppte sich als optimale Polymerzusammensetzung. 30 µl dieses Polymers bei 1500 rpm Rotationsgeschwindigkeit und 5 s Rotationszeit mittels Spin Coating auf die QCMs aufzutragen stellte sich als optimal heraus. Sensoren, die unter optimierten Bedingungen hergestellt wurden, zeigten allerdings keine Selektivität gegenüber den Referenzorganismen *Escherichia coli* und *Bacillus cereus*, da die Signalintensität für die Referenzorganismen bis zu 3 mal höher war als für den Analyt. Daher wurde das eingesetzte Polymer gegen Polymethacrylsäure getauscht.

Für Polymethacrylsäure beinhalteten Optimierungsexperimente Schichtdickenbestimmungen und Entfernungversuche der Mikroorganismen, da die Zusammensetzung des Polymers nicht variiert wurde. Die optimierten Herstellungsparameter waren 10 µl 1:4 verdünnte Polymerlösung bei 3000 rpm Rotationsgeschwindigkeit und 5 s Rotationszeit mittels Spin Coating auf die QCMs aufzutragen. Außerdem wurden Stempel durch Immobilisierung der Bakterien mittels APTES hergestellt, allerdings zeigte das Prägen mit diesen Stempeln keinen Erfolg. Dennoch konnten funktionstüchtige Sensoren mit der Sedimentationsprägemethode erzeugt werden, welche auf die Parameter Sensitivität, Selektivität, Reversibilität und Stabilität erfolgreich getestet wurden. Dabei konnten Sensitivitäten von $4,5 \cdot 10^6$ Zellen/ml erreicht werden.

Außerdem zeigten die *S. epidermidis* Lösungen ein bis zu 70-mal stärkeres Signal als Lösungen von *B. cereus* und *E. coli*.

Abschließend wurde ein neuer Erkennungsmechanismus postuliert als auch ein Ausblick über zukünftiges Entwicklungspotential dargeboten.

Table of contents	Page
1. INTRODUCTION.....	7
2. THEORETICAL BACKGROUND.....	8
2.1. CHEMICAL SENSORS	8
2.2. MASS-SENSITIVE SENSORS	10
2.2.1. <i>Piezoelectric effect</i>	10
2.2.2. <i>Quartz crystal microbalance</i>	11
2.2.3. <i>Measuring principle</i>	13
2.2.4. <i>Calculation of layer thicknesses</i>	15
2.3. MOLECULAR IMPRINTING	16
2.4. MOLECULAR IMPRINTING TECHNIQUES	17
2.4.1. <i>Volume imprinting – Bulk imprint</i>	17
2.4.2. <i>Surface imprinting</i>	18
2.4.2.1. <i>Stamp imprinting</i>	19
2.4.2.2. <i>Sedimentation imprinting</i>	20
2.5. STAPHYLOCOCCUS EPIDERMIDIS	21
2.6. NETWORK ANALYZER	22
2.7. OPTICAL MICROSCOPY.....	23
2.8. ATOMIC FORCE MICROSCOPY	26
2.9. ALTERNATIVE DETECTION METHODS FOR BACTERIA	28
3. EXPERIMENTAL	29
3.1. MATERIALS	29
3.2. EXPERIMENTAL PROCEDURES.....	29
3.2.1. <i>Bacteria cultivation</i>	29
3.2.2. <i>Device manufacturing and characterization</i>	30
3.2.3. <i>Imprinting protocols</i>	33
3.3. STABILITY STUDY OF FROZEN BACTERIA SOLUTION.....	34
3.4. POLYMER SCREENING BY QCM MEASUREMENTS	34
3.5. POLYURETHANE	36
3.5.1. <i>First polyurethane QCM measurements</i>	36
3.5.2. <i>Polyurethane screening on glass slides</i>	36
3.5.3. <i>Determining the layer heights of PUEq</i>	37
3.5.4. <i>Template removal from PUEq</i>	38

3.5.5. QCM measurements	39
3.6. POLYMETHACRYLIC ACID	40
3.6.1. Determining the layer heights of PA2THF	40
3.6.2. Template removal from PA2THF	40
3.6.3. APTES stamp imprint	40
3.6.4. QCM measurements	41
4. RESULTS AND DISCUSSION.....	42
4.1. STABILITY STUDY OF FROZEN BACTERIA SOLUTION.....	42
4.2. POLYMER SCREENING BY QCM MEASUREMENTS	46
4.3. POLYURETHANE	49
4.3.1. First polyurethane QCM measurements	49
4.3.2. Polyurethane screening on glass slides	50
4.3.3. Determining the layer heights of PUEq.....	54
4.3.4. Template removal from PUEq	56
4.3.5. QCM measurements	58
4.4. POLYMETHACRYLIC ACID	60
4.4.1. Determining the layer heights of PA2THF	60
4.4.2. Template removal from PA2THF	61
4.4.3. APTES stamp imprint	63
4.4.4. QCM measurements	66
4.4.5. PA2THF Sensor characteristics.....	67
5. CONCLUSION.....	72
5.1. SUMMARIZED CONCLUSION	72
5.2. PROSPECTS	73
6. UNITS AND ABBREVIATIONS	74
6.1. ABBREVIATIONS:.....	74
6.2. UNITS:.....	75
7. REGISTERS	76
7.1. FIGURE REGISTER	76
7.2. TABLE REGISTER	78
7.3. EQUATION REGISTER	78
8. REFERENCES	79

1. INTRODUCTION

Terrorism is an increasing threat to the civilian population of European countries, as the number of terrorist attacks has increased during the last decade. Newspaper reports, newscasts on television or articles on the internet regularly report on new attacks now. Therefore it is easily understood that the fear of terrorism also increases. A lot of these attacks were carried out using explosives or firearms as tools of death and destruction [1], but food and water supply chains are other possible targets for terrorists. These are, of course, not easily destroyed by explosives, but can spread death and illness for millions if contaminated with chemical, radioactive or biological agents [2].

Especially biological toxins produced by microorganisms can be very dangerous to human health as well as difficult to be detected in time. It is therefore inevitable to develop a tool for continuous, fast and sensitive detection of potentially dangerous microorganisms in water supply chains or in food.

The bacterium *Staphylococcus epidermidis*, a skin colonizing microorganism that is harmless to humans under normal conditions is one possible biological weapon: It can become quite dangerous as a potential pathogen when introduced into fresh or open wounds, as it is the major cause for wound infections in hospitals and healthcare centers [3]. Its ability to build a biofilm and its resistance to the majority of antibiotics makes the spherical shaped microorganism even more dangerous. Furthermore *S. epidermidis* is a natural survival artist as it endures several days at temperatures around -20 °C and storage in distilled water (section [3.3]). It is therefore of utmost interest to develop a fast and reliable sensor for the detection of *S. epidermidis*, as the organism itself is dangerous to human health on the one hand, and as the sensor principle may be applicable to other, even more threatening microorganisms.

Therefore both fast detection and low production costs are required for the sensor needed. The quartz crystal microbalance (QCM) a mass-sensitive device consisting of a gold coated quartz wafer and a sensitive layer, occurs as possible solution to the task [4]. It is cheap, easily produced and, depending on the sensitive layer, fast and selective.

This master thesis is part of an EU project and tackles the principal production steps, optimization and first evaluation of a QCM sensor for the detection of *S. epidermidis* in aqueous solution as an in situ screening tool for water supplies.

2. THEORETICAL BACKGROUND

2.1. Chemical sensors

According to the International Union of Pure and Applied Chemistry (IUPAC) a chemical sensor is defined as: “... a device that transforms chemical information, ranging from the concentration of a specific sample component to total composition analysis, into an analytically useful signal. The chemical information, mentioned above, may originate from a chemical reaction of the analyte or from a physical property of the system investigated.” –IUPAC 1991. [5]

The range of chemical information is therefore not limited and may consist of detecting color using nothing more than a simple device, such as a camera or a photometer. However, it may also mean complete separation, identification and quantification of a mixture of complex, biological substances. Therefore it is necessary to define chemical sensors in some more detail, at least for this work. A chemical sensor should therefore have the following attributes:

- The response time should be reasonably fast.
- The chemical information should be transformed into an electrical signal.
- The sensor should be selective for the target analyte.
- The signal or response should be reversible.
- The sensor itself should be long lasting and sustainable.
- The sensor should be miniaturized.
- The detection limit should be as low as possible.

Sustainability and long term stability of a sensor are not always necessary, especially if the device itself is rather cheap to produce. In such cases the sensor can be replaced easily at low costs.

The principal design of a chemical sensor is given in Figure 1. It consists of a sensitive layer, a transducer and the data recording and evaluation system. This layer can consist of a variety of materials (e.g. polymers, biochemical layer, membranes) and may take on different forms (e.g. nanoparticles, thin layers, electrodes) to fit the need of analysis. It constitutes the selective part of the device. Ideally the analyte binds reversibly to the sensitive layer hence creating a chemical signal, which is then transformed into an analytically useful, electronic signal by the transducer. This transducer, however, is not selective and transfers every chemical signal into an electronic one. The data recording and evaluation system records the signal and enables the analyst to evaluate the information obtained. In most cases this system is a personal computer, equipped

with appropriate data analysis software. Many a time an electrical system is needed between the computer and the transducer to obtain the best data transfer possible.

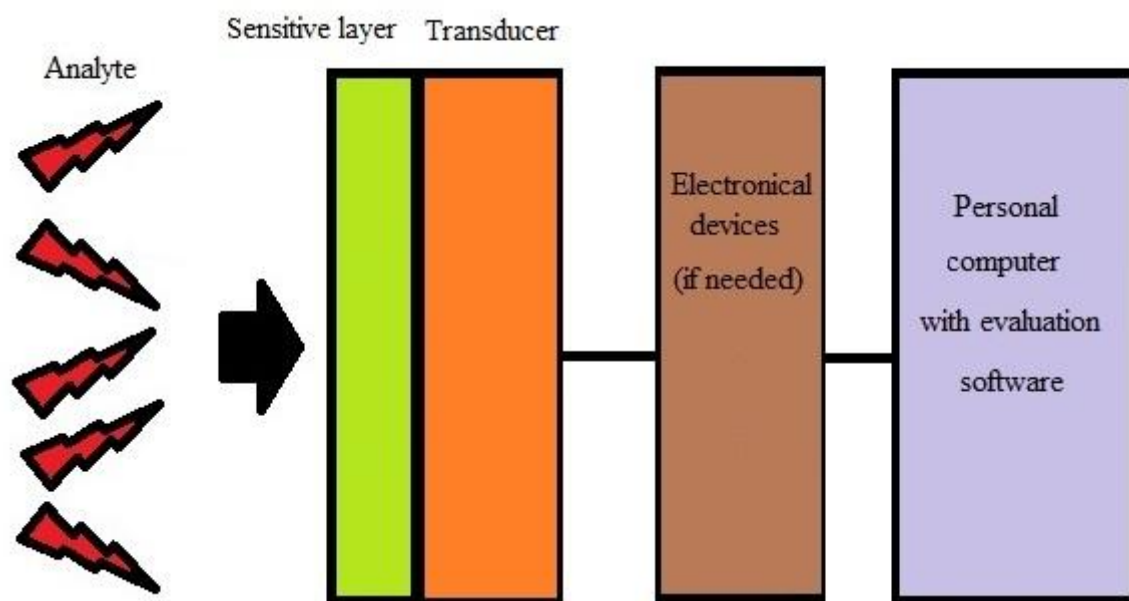


Figure 1: Schematic general sensor setup

Due to the substantial progress in many different scientific fields, such as healthcare, industry or ambient surveillance, the need for rapid analysis with miniaturized devices has grown and opened up many a possibility for chemical sensor applications, such as point-of-care patient monitoring in clinical applications, process monitoring, and control in industry or detection of chemical, biological and toxin warfare in military and defense applications [6]. This high need created a large variety of chemical sensors, hence making it necessary to categorize devices into groups. The IUPAC classifies the sensors by the working principle of the transducer and separates them into the following classes [5]:

- Optical devices measuring for example absorbance or light scattering.
- Electrochemical devices, such as potentiometric sensors or electrochemical electrodes.
- Electrical devices, mostly using semiconductor technologies.
- Magnetic devices, based on the change of magnetic properties in analytes.
- Thermometric devices, measuring heat effects of chemical reactions.
- Mass-sensitive devices, such as the quartz crystal microbalance or the surface acoustic wave sensor.

Another special group of sensors are so-called biochemical sensors, which make use of specific biochemical reactions in the sensitive layer to generate signals. An example of such a

biochemical sensor is the pregnancy test, which detects hCG-antigens in urine. As this work mainly relies on QCM measurements, the following sections will discuss mass-sensitive devices in some more detail.

2.2. Mass-sensitive sensors

2.2.1. Piezoelectric effect

Mass-sensitive sensors are, in principle, small balances which respond to mass differences on the surface of the transducer. The so called reciprocal piezoelectric effect is the main physical phenomenon used to sense mass changes. It is the inverse effect of the piezoelectric effect, which describes induction of surface voltage in a crystal when applying force to the material. This voltage is induced through shifts of centers of gravity of the charge inside the material and was first described by Jacques and Pierre Curie in 1880 [7].

The reciprocal piezoelectric effect describes induction of mechanical deformation by applying voltage to the crystal, which furthermore can be used for detecting even very small masses in the ng range. The piezoelectric effect is shown in Figure 2, where force is applied on a crystal with no center of symmetry to separate charges and thus create surface voltage. Quartzes are one of many inorganic crystals that contain centers of gravity of the charge and no inversion center and can therefore be the source of piezoelectricity.

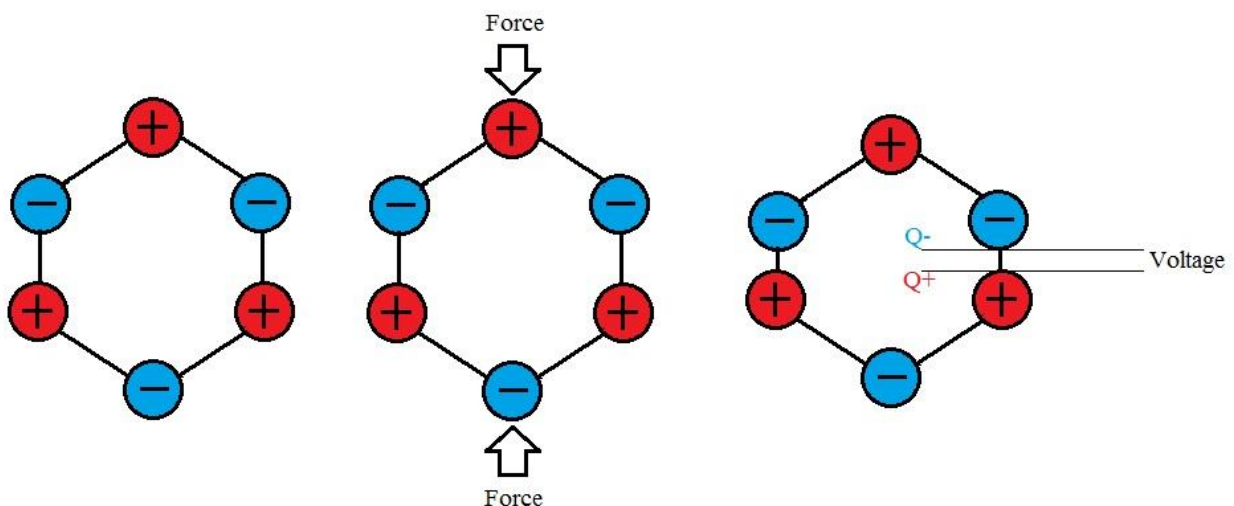


Figure 2: Piezoelectric effect, scheme

But also organic nanostructures show piezoelectricity, such as diphenylalanine peptide nanotubes, as shown by Kholkin et al [8]. Piezoelectric mass sensors can be used for a variety of

applications such as biosensors [9] or for studying complex biomolecular systems at the solution-surface interfaces [4]. The system used in the present work is the quartz crystal microbalance (QCM), which will be explained subsequently.

2.2.2. Quartz crystal microbalance

The quartz crystal microbalance (QCM) is a piezoelectric device capable of measuring very small changes in mass loading on top of the quartz crystal. It is therefore very useful as a mass sensor. Unlike the elements in section [2.2.1], QCM uses the piezoelectric effect not to generate voltage but uses applied voltage to generate movement, especially vibration. The different modes of bulk vibration of a quartz plate are shown in Figure 3.

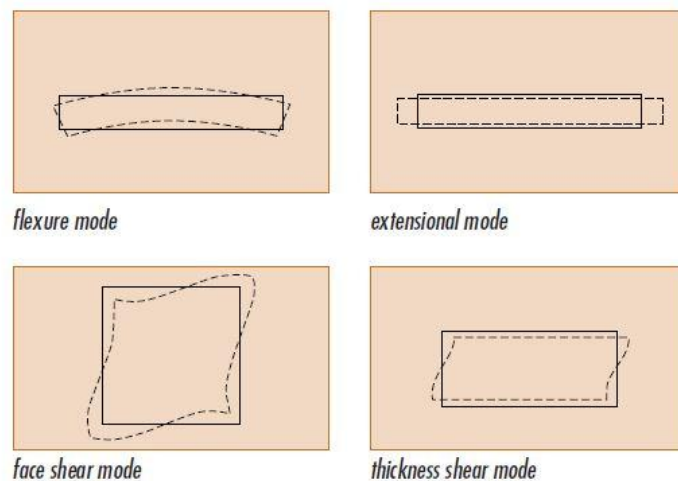


Figure 3: Modes of vibration for an AT-cut quartz crystal; copyright by Jauch Quartz GmbH, 2007.

Quartz is the most commonly used material of all piezoelectric substances and is “... used to generate frequencies to control and manage virtually all communication systems” –Jauch Quartz GmbH, 2007 [10]. The fast development of electronical devices using quartz oscillation led to increased need in both quality and amount of quartz crystals. This demand could not be satisfied with natural quartz. Therefore hydrothermal synthesis for mass producing of α -quartz was established in 1950 [11]. After synthesis the quartz crystal is cut in a certain way to obtain quartz plates of different geometry and with different properties. Each mode of vibration results from a defined optimal cutting angle, which leads to a large variety of possible applications of the final substrates. The vibration used in QCMs is the thickness shear mode, which can be realized by using AT-cuts. Different cutting methods are shown in Figure 4.

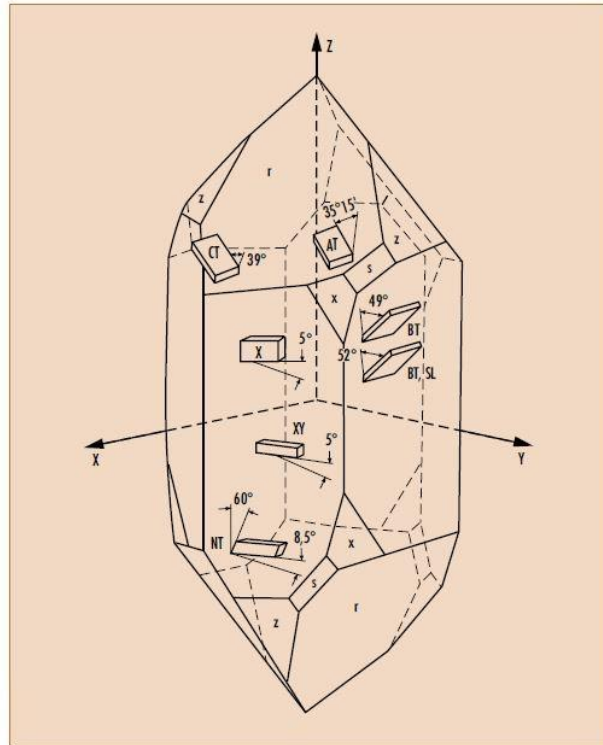


Figure 4: Different angles of cutting a quartz crystal; copyright by Jauch Quartz GmbH, 2007.

The thickness shear mode of vibration is very resistant against environmental influences such as temperature change and is therefore suited for sensor applications. The fundamental shear mode of QCMs can be used until up to 20 MHz, frequencies higher than this can be realized by using the third overtone thickness shear mode [10]. In this work AT-cut, circular quartz wafers with a frequency of about 10 MHz were used for all experiments. This corresponds to a wafer thickness of 168 μm .

2.2.3. Measuring principle

In order to generate an analytically useful signal, analyte concentration and detectable signal must be correlated. In case of QCMs this context is the frequency shift of the substrate depending on mass loading, which was first described by G. Sauerbrey in 1959 [12]. He found that the frequency of a quartz plate changed depending on the amount of mass on top of it and described the correlation of frequency change and mass change by the so called Sauerbrey equation (Equation 1):

$$\Delta f = - \frac{2f_0^2}{A\sqrt{\rho_q \mu_q}} \Delta m$$

Equation 1: Sauerbrey equation

Δf Frequency change

Δm Mass change

f_0 Resonant frequency

A Piezoelectrically active area

ρ_q Density of quartz

μ_q Shear modulus of quartz for an AT-cut crystal

It can clearly be seen that the correlation between frequency and mass change is linear as f_0 , A and the term underneath the square root are constant for a given QCM. This equation is only valid for measurements in gas phase and only if frequency changes are not higher than 2 % of the fundamental frequency. In order to use QCMs in liquid phase, the equation has to be adapted for liquid measurements as follows in Equation 2:

$$\Delta f = -f_0^{\frac{3}{2}} (\eta_l \rho_l / \sqrt{\rho_q \mu_q})^{1/2}$$

Equation 2: Kanazawa - Gordon equation

Δf Frequency change

f_0 Resonant frequency

ρ_l Density of the liquid solution

η_l Viscosity of the liquid solution

ρ_q Density of quartz

μ_q Shear modulus of quartz for an AT-cut crystal

This extension of the Sauerbrey equation was introduced by Kanazawa and Gordon in 1985 and makes it possible to use QCMs in liquid phase [13]. The influence of viscosity is rather low compared to the influence of mass change, but can still lead to signal drift over time: as viscosity changes with temperature and the temperature inside the measurement system increases due to the movement of the quartz plate.

As the equations show, QCMs can be used for detection in both liquids as gases, but the resonators themselves are not selective, because the frequency changes due to any mass change. It is therefore inevitable to create selectivity on the quartz wafer surface.

Furthermore the change in frequency depends on the resonant frequency of the quartz; hence the signal can be increased by increasing the resonant frequency of the substrate. However, that parameter is limited by the thickness of the quartz crystal. Therefore a trade-off between signal intensity and stability of the QCM has to be accepted.

The piezoelectrically active area A is the area in between two gold electrodes on the top and bottom side of a quartz crystal wafer. The geometry of the electrodes is shown in Figure 5.

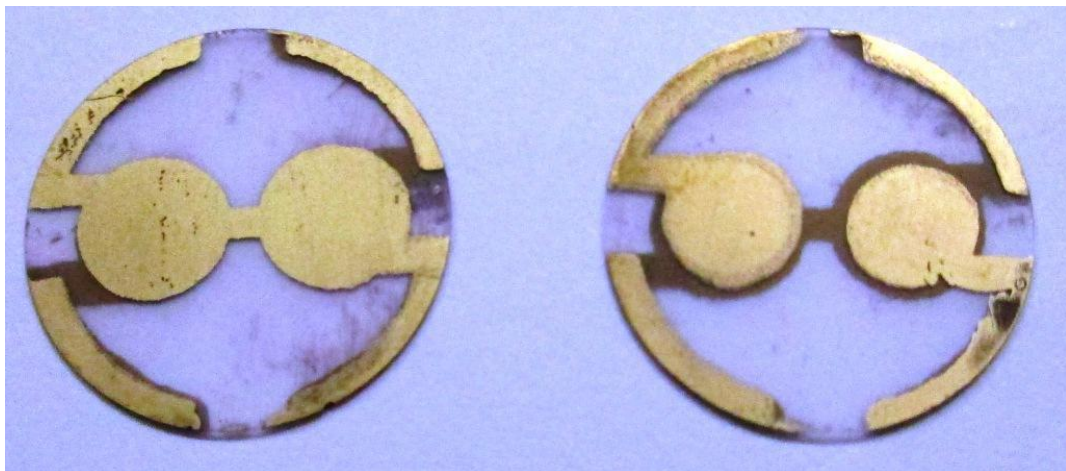


Figure 5: Gold electrodes on a QCM; Left: top-side electrode; Right: bottom-side electrode

2.2.4. Calculation of layer thicknesses

If the quartz crystal itself is coated with electrode structures and the thickness shear frequency of the area in between the electrodes can be measured, the Sauerbrey equation [Equation 1] can be converted into the equation shown in Equation 3:

$$\Delta m = -\Delta f A \frac{\sqrt{\rho_q \mu_q}}{2f_0^2}$$

Equation 3: Modified Sauerbrey equation

Δf Frequency change

Δm Mass change

f_0 Resonant frequency before mass loading

A Active piezoelectric area

ρ_q Density of quartz

μ_q Shear modulus of quartz for an AT-cut crystal

This equation allows calculating mass loading on top of the QCM electrodes and therefore enables us to determine the success of different preparation steps carried out on QCMs. For instance, layer height is a very important parameter when using molecularly imprinted polymer layers. In order to determine this, one has to know polymer density. The calculated mass is then divided by density and afterwards by the piezoelectrically active area, which finally leads to layer thickness LT according to Equation 4.

$$LT = \frac{\Delta m}{\frac{\rho_p}{A}}$$

Equation 4: Formula for the layer thickness calculation

ρ_p Density of the polymer

LT Layer thickness

Δm Mass change

A Piezoelectrically active area

As the piezoelectrically active area appears in both, numerator and denominator, it can be cancelled and hence needn't be known. This leads to an equation for determining layer thickness as follows in Equation 5:

$$LT = -\Delta f \frac{\sqrt{\rho_q \mu_q}}{2f_0^2 \rho_P}$$

Equation 5: Final formula for the layer thickness determination

- Δf Frequency change
- f_0 Resonant frequency before mass loading
- A Active piezoelectric area
- ρ_q Density of quartz
- μ_q Shear modulus of quartz for an AT-cut crystal

This equation was used for calculating all layer thicknesses in this work. Densities of the polymers were obtained from different sources [14] [15], the values of the density of quartz and the shear modulus of quartz for an AT-cut crystal were obtained from [12] and the frequencies needed were measured using a network analyzer. As the densities of the polymer layers change depending on process parameters and their porosity, the values calculated are not exact and only indications for the real values.

2.3. Molecular imprinting

Compared to other recognition techniques molecular imprinting is a fairly easy way to create materials for different possible usages by creating cavities inside or on the surface of a substrate. These cavities are equipped with specific chemical recognition sides. G. Wulff, for example, postulated in 1995 that molecular imprinting of cross linked polymers could be a way to create artificial antibodies [16]. Molecular imprinting has also been used to improve separation in chromatography, as by F. Omid to determine 4-Chloro-2-Methylphenoxy Acetic Acid in complex matrices [17]. But not only small molecules (like this one), or proteins [18] can be detected, but also whole cells or bacteria as, for example, described by Lopez et al in 2003 [19]. M. Lopez also describes the need for fast detection of different harmful viruses and bacteria for the safety of agricultural growth, which demonstrates the usefulness of molecularly imprinted

polymers for sensor applications and analytics. Several techniques exist to create a molecularly imprinted polymer (MIP).

2.4. Molecular imprinting techniques

Before describing different ways of creating the above mentioned cavities, the recognition mechanism of MIP has to be explained. The polymer itself consists of three major components, firstly the functional monomer(s), secondly the cross linker, and thirdly the solvent.

The functional monomer is a substance with two major attributes: its ability to build a polymeric chain and a functional group that interacts in an exactly defined way with the analyte, for example via hydrogen bonding, Van-der-Waals interactions or hydrophobic interactions. It is of utmost importance for successful imprinting that the interactions between monomer and analyte are reversible, hence non-covalent. Therefore the functional monomer has to be chosen carefully for each analyte. Sometimes polymerization of the monomer does not start by thermal or UV activation, hence a catalyst or initiator has to be added to the mixture [20].

The purpose of the cross linker is to generate cross linked connections to the monomer in order to avoid linear chain polymerization, because chains would not lead to the desired mechanical properties, such as ruggedness or stability against solvents or detergents.

The solvent also needs to be chosen thoughtfully, because on the one hand it must be able to dissolve all substances needed for polymerization and on the other hand it needs to fulfil certain requirements concerning volatility depending on the subsequent processing of the polymer [16].

There are many ways of molecular imprinting and therefore only the ones important for this work will be explained here. Classical bulk imprinting will be presented first, because it is, in a way, the “reference method”. Afterwards surface imprinting will be discussed together with the reasons to rely on them during the work of this thesis.

2.4.1. Volume imprinting – Bulk imprint

Volume or bulk imprinting is the most straightforward way of imprinting an analyte into a polymer. The template is added to the mixture of functional monomer, cross linker and solvent. The liquid is then coated onto the substrate. During polymer hardening the functional groups of the monomer assemble around the template in a thermodynamically preferred way generating a cavity that can then selectively bind the analyte. Polymerization can be initiated by temperature,

UV light or a catalyst / initiator and takes a long or short time depending on the polymer system used. After complete hardening the template can be removed by washing or evaporation and leaves behind cavities suitable for rebinding the analyte [21]. A schematic diagram of the bulk imprinting process is shown in Figure 6.

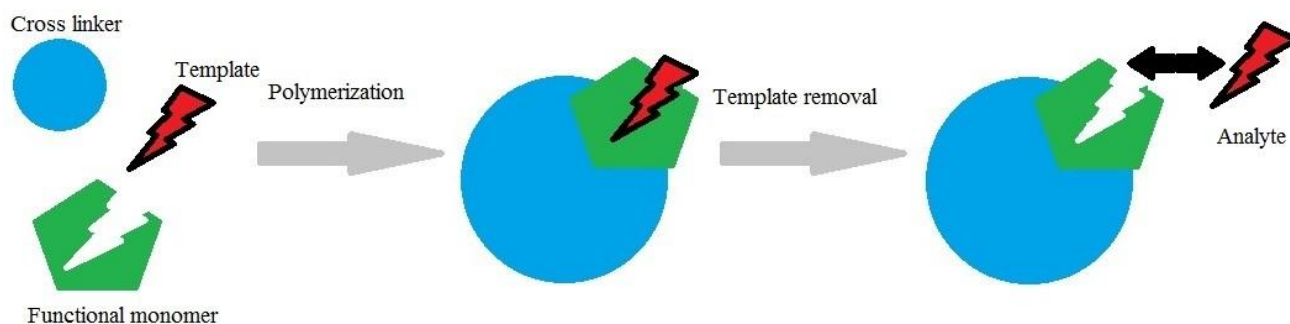


Figure 6: Scheme of the bulk imprinting method

Volume imprinting is straightforward and efficient, creating cavities not only on the surface of the polymer layer but everywhere inside it, which is as well an advantage as a disadvantage. The advantage of cavities generated in every part of the layer is that one can create a larger amount of recognition sites and that the cavities are partly surrounding the analyte as a whole, hence creating stronger analyte – cavity binding and therefore larger signals. Due to hardening conditions (UV light or heat) the method is not suitable for templates unstable to UV or higher temperatures, hence creating the need for proper investigation if the polymer system chosen is suitable for the target analyte. Furthermore the polymer must be porous in order to allow diffusion of the analyte into the cavities and the analyte has to be small enough to pass through the pores of the polymer. Therefore, bulk imprint is only suitable for small analytes and not for the bacteria targeted in this work.

2.4.2. Surface imprinting

Surface imprinting methods do not require presence of the template during pre-polymerization and are therefore suitable for delicate analytes, such as biological substances (e.g. proteins or enzymes) or living cells. However, surface imprinting requires the analyte to be pressed into the polymer one way or the other and therefore, as the name already suggests, only creates cavities on the surface of the polymer, leading to fewer cavities in total. There are two major surface

imprinting techniques that have been used in this work, namely stamp imprinting and sedimentation imprinting.

2.4.2.1. Stamp imprinting

The most commonly known surface imprinting method is the so called stamp imprint. Prior to imprinting the template, a suitable stamp has to be created by immobilizing it on a substrate. This can be quite challenging depending on both, the surface for immobilization and the target analyte, because the substance of interest needs to be bound irreversibly onto the surface but is also required to maintain its original shape in order to create cavities properly representing the steric and functional properties of the template. A schematic picture of the stamp imprint is shown in Figure 7.

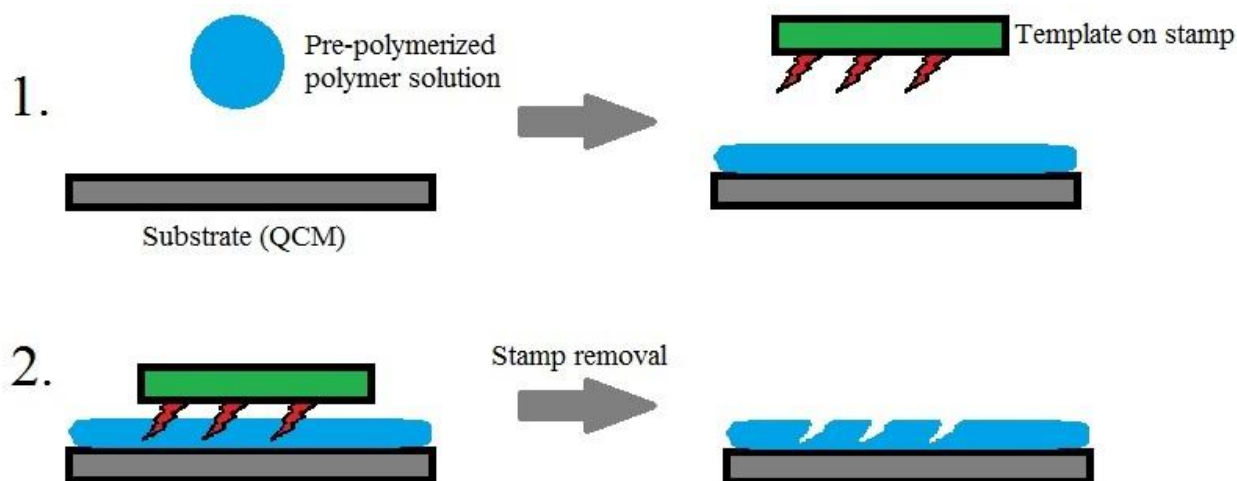


Figure 7: Scheme of the stamp imprinting method

If a suitable stamp is found, imprinting itself is fairly easy: The polymer is pre-polymerized up to a point where it is still soluble and fluid. The solution is then coated onto the substrate (e.g. the QCM) by spin coating or similar techniques. Then the stamp is firmly pressed into the still wet polymer. While the stamp – polymer – substrate sandwich is left hardening, the functional groups self-assemble around the template and give rise to the respective selective recognition cavities. Afterwards the template is easily removed from the polymer by cautiously removing the stamp. The substrate can be used immediately [22].

2.4.2.2. Sedimentation imprinting

Sedimentation imprinting is the second surface imprinting method utilized for this thesis and offers both advantages and disadvantages compared to stamp imprinting. In a first step the pre-polymerized polymer solution is once again coated onto the substrate or QCM. After spin coating a template suspension (or solution) is placed on top of the pre-formed oligomer film and firmly pressed into it by a suitable squeezer (in this work the squeezer is a rectangular piece of polydimethylsiloxane PDMS). The sandwich is then left for complete hardening by thermal activation, as before. Sedimentation imprinting is shown schematically in Figure 8.

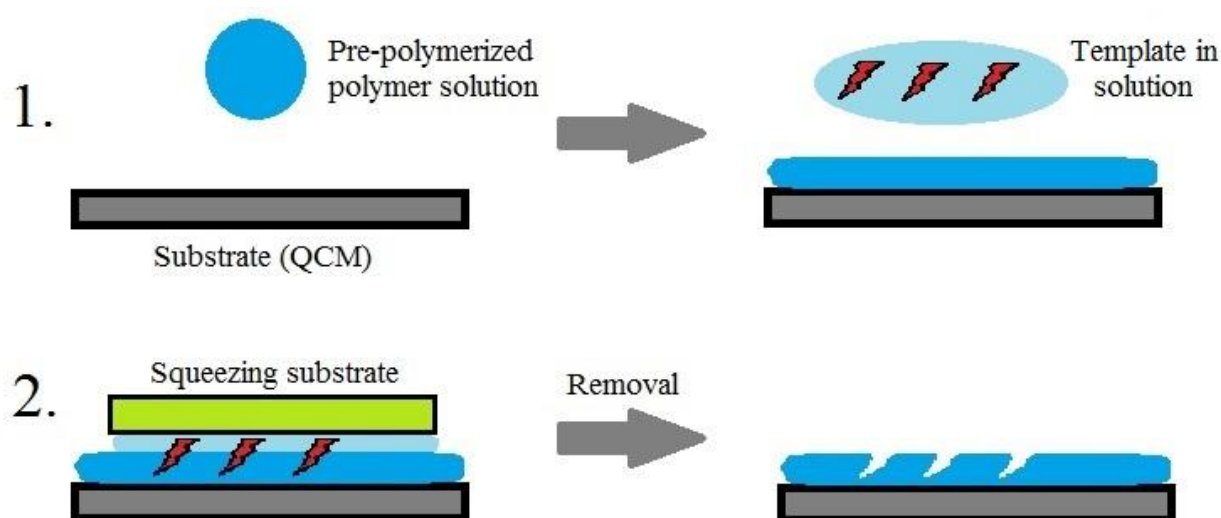


Figure 8: Scheme of the sedimentation imprinting method

Sedimentation imprinting offers huge advantages: On the one hand it is not required to immobilize the analyte on top of a substrate, and on the other hand the analyte can be used in solution, which facilitates handling. Furthermore removing the stamp in stamp imprinting can damage the polymer surface, because the template species are either physisorbed on its surface or even chemically bound, hence destroying the cavities. Some disadvantages, however, include incomplete removal of the template after imprinting, because it can bind irreversibly to the polymer during hardening. Furthermore solubility of the polymer in the solvent used for the analyte has to be considered in order to not dissolve the polymer during imprinting [23]. As has been demonstrated, sedimentation imprinting is a gentle method for creating cavities on the surface of a polymer and is therefore inherently well suited for a delicate analyte, such as *S. epidermidis*.

2.5. Staphylococcus epidermidis

S. epidermidis is a potentially pathogenic, colonizing bacterium on the human skin [3] that was first discovered in 1884 by Friedrich Julius Rosenbach, who named it *Staphylococcus albus* [24]. Even though nosocomial infections caused by this bacterium have gained substantial attention, it is actually not infectious for humans with a fully functioning immune system. If, however, the immune system is weakened by a disease or invasive surgery, it can cause both general and post-surgical wound infections. Due to its natural environment, the skin of mammals and especially humans, *S. epidermidis* became resistant to different antibiotics such as penicillin and methicillin, hence turning it into a MDR, a multi drug resistant, microorganism. It is, however, usually pathogenic, as it maintains a symbiotic relationship with its host: Spreading dominantly across the parts of the human skin it colonizes, it keeps other microorganisms away that could produce aggressive infectious substances [25]. In order to build up such dominance and to survive the human immune system, *S. epidermidis* had to develop several mechanisms of survival, one being the ability to build biofilms or at least biofilm-like aggregates [26]. This tendency to agglomerate can clearly be seen when watching the vivid cells in a light microscope. The bacteria normally come at least in twos, as can be seen in Figure 9 and Figure 10.

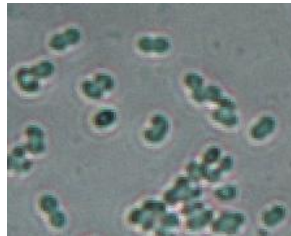


Figure 9: *S. epidermidis*, optical microscope image; 1000 times magnification



Figure 10: *S. epidermidis*, AFM image

The upper picture shows the cells of *S. epidermidis*, using a light microscope with 1000 times magnification, the lower picture shows a section of an AFM measurement of the microorganism. The tendency to agglomerate, especially on plastic surfaces, leads to further problems with regard to nosocomial infections, as *S. epidermidis* form biofilms on catheter tubing leading to urinary tract infections [3], or on artificial prostheses leading to inflammatory infections.

S. epidermidis is spherical, between 0.5 and 1.0 μm in diameter [26] and has a generation time of 44 minutes at 37 °C in a PET tube in growth medium [27]. The cells are coagulase negative, gram positive and show high diversity with 74 identified sequence types, most of which show the ability to form biofilms and all of which tend to agglomerate. Interestingly the human body seems to tolerate *S. epidermidis* on its skin in general, but not everywhere. Aswani et al. found that there are bacteriophages in the anterior human nares, defending the respiratory system against *S. epidermidis* and thus regulating the fauna of microorganisms living inside the nares.

2.6. Network Analyzer

The frequency of the electrodes on a QCM can easily be determined by a so called network analyzer. Among others, accurately determining resonance frequencies of the pure device (i.e. without the oscillator circuit) is necessary in order to determine layer thicknesses of polymer coatings or imprints, as the change in frequency is related to a change in mass loading, as discussed in section [2.2.3].

In the simplest case a network analyzer generates a sinus shaped signal which is then induced into the device under test (DUT), in this case the QCM. The change of the signal produced by the device is measured. The sinus shaped response of the DUT differs both in amplitude and phase from the exciting signal. Modern network analyzers can capture both differences as a complex variable and can therefore express the S – parameters in a complex way. The S – parameters, or scattering parameters, are a matrix of arguments that describe the electrical behavior of a linear electrical network when undergoing different steady state stimulations. One of those parameters is, in the case of QCMs, the frequency of the thickness shear modes of the area in between the two electrodes [28]. The used network analyzer, measuring a quartz device, is shown in Figure 11.

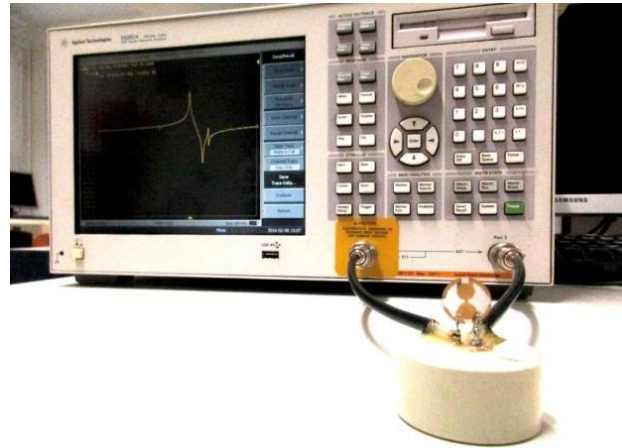


Figure 11: Agilent 8712ET network analyzer

The network analyzer records damping of the QCM as a function of its frequency. Damping describes the ratio of the ingoing signal compared to the resulting signal after passing the DUT and is given in decibel [dB] and is related to impedance. With increasing mass loading or defective gold electrodes, damping of the QCM increases. Therefore high damping indicates both high mass loading and insufficient electrode quality.

As the QCMs are undergoing a variety of preparation steps that change the mass loading on the electrodes, it is necessary to measure the devices before and after each step to determine the success of all preparations.

2.7. Optical microscopy

The optical or light microscope is an instrument capable of showing an enlarged picture of a very small object making use of a system of lenses and a light source beneath the object. The effect of enlargement of objects seen through a spherical glass vessel filled with water was already described by Seneca around 4 BC [29]. Even though first optical auxiliaries, such as magnifying glasses, were invented quite early, it took a long time from Seneca to the first microscope. Even though the records at the time were already quite good, it is not easy to say who invented the first microscope. Galileo Galilei build a compound microscope to magnify pictures of insects and other objects visible to the human eye in 1602, but not in order to study the microscopic world but in order to proof his concept of picture enlargement by using two lenses, which he actually used to build a telescope. Another candidate for the title “inventor of the microscope” could be the Dutch instrument maker Cornelius Drebbel (1572 to 1623). His biographers claim that he

invented the first microscope earlier than Galilei, even though there is only evidence that he built microscopes, but none that he invented them [29].

Nevertheless the light microscope became a very popular instrument for investigating biological substrates and was also used in this work to examine the behavior of *S. epidermidis*. The principal setup of a compound light microscope is shown in Figure 12:

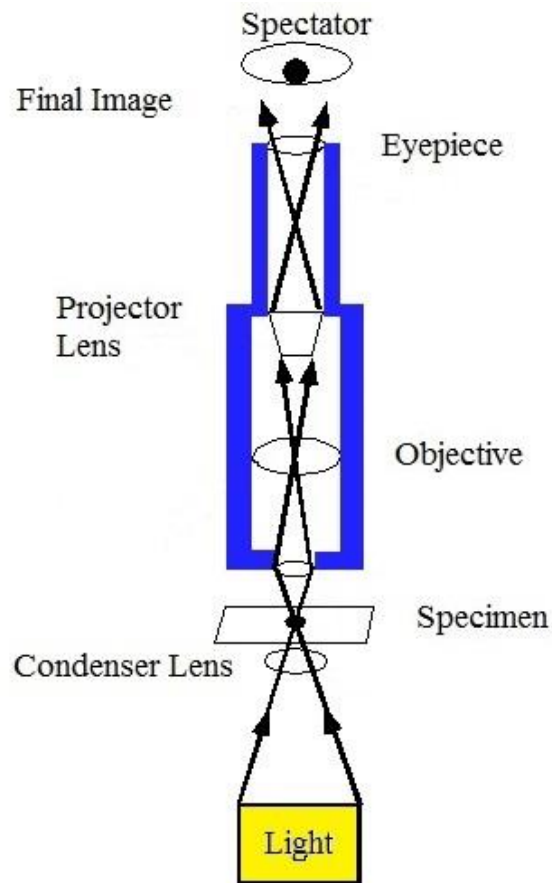


Figure 12: Principal setup of an optical microscope

As light travels past or through the specimen, it is focused by the objective and the projector lens. This enlarges the viewing angle, which generates an enlarged image of the specimen. The effect of enlarged images due to enlarged angles was already described by Euclid about 300 BC [29] and can easily be observed when watching a large object like a building or a tree from either far away or a close distance. When being close to the big object, the angle of light hitting the eye becomes big and the object appears larger. If watched from a higher distance, the angle of incident light becomes smaller and the object also appears to be less in size.

The resolution of microscope images is given by the Rayleigh criterion, which was found in 1879 by John William Strutt, 3. Baron Rayleigh [30]. It says that images of light radiating points are actually diffraction patterns. In the layer of the pattern with the highest intensities, two points can only be separated if the intensity maximum of one point is situated in the intensity minimum of the other point.

The Rayleigh criterion, however, does not come in very handy when one wants to evaluate the resolution of the microscope used in the lab. Therefore it is easier to determine the full width at half maximum (FWHM) value of the point spread function, which describes the three dimensional picture of a light radiating point created by microscopic observation. The formula to determine the FWHM value for the x, y directions is given in Equation 6:

$$FWHM = \frac{0.51 \lambda}{NA}$$

Equation 6: FWHM formula

λ Wavelength of used light

NA..... Numerical aperture

FWHM Full width at half maximum

The numerical aperture is a value specific for the microscope or rather for the lenses used and represents the range of angles under which the system can collect or emit light; it is constant for each microscopic system. The formula also contains the wavelength of used light, which indicates that the limits of resolution depend on the light source used [31].

The possible resolution of the optical microscope used in this work is approximately 0.2 μm , which is just enough to detect *S. epidermidis* with its diameter of at least 0.5 μm , as was already mentioned before. An exemplary picture of the living bacteria taken with the optical microscope used in this work with 1000 times magnification is shown in Figure 13.

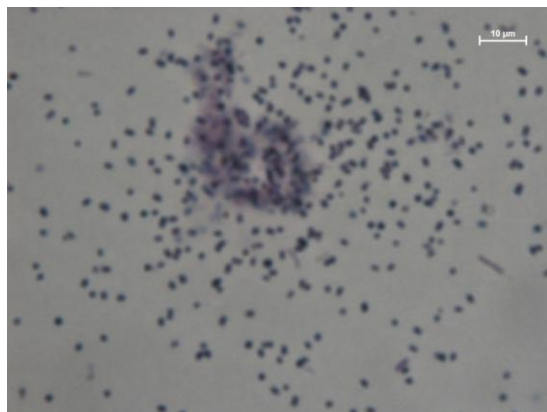


Figure 13: Microscopic image (magnification 1000 times) of *S. epidermidis*

2.8. Atomic force microscopy

Atomic force microscopy (AFM) is a surface imaging technique making use of attractive and repulsive forces of matter and can therefore reach resolutions of less than one nanometer, which is more than 1000 times better than any optical microscope. It was invented in 1985 by Binnig et al. [32] and has since then gained outstanding popularity for characterizing surfaces and surface reactions.

An AFM works as follows: A very small tip with a minimum diameter of 1 nm placed on a lever is positioned close enough to the surface of the sample in order to generate repulsion and attraction on the atomic scale. This lever, called cantilever, is then moved over the surface and the forces acting between tip and substrate influence deformation of the lever in a similar way as forces of a certain weight influence deformation of a spring. This deformation can then be measured and correlated to surface topography [32]. At the beginning this was done using a scanning tunneling microscope (STM), but in 1988 a system using a weak laser and a position-sensitive detector was introduced [33]. In this work only AFM using a laser as sensing device was applied, therefore STM will not be discussed in detail. Figure 14 shows the schematic structure of the AFM used:

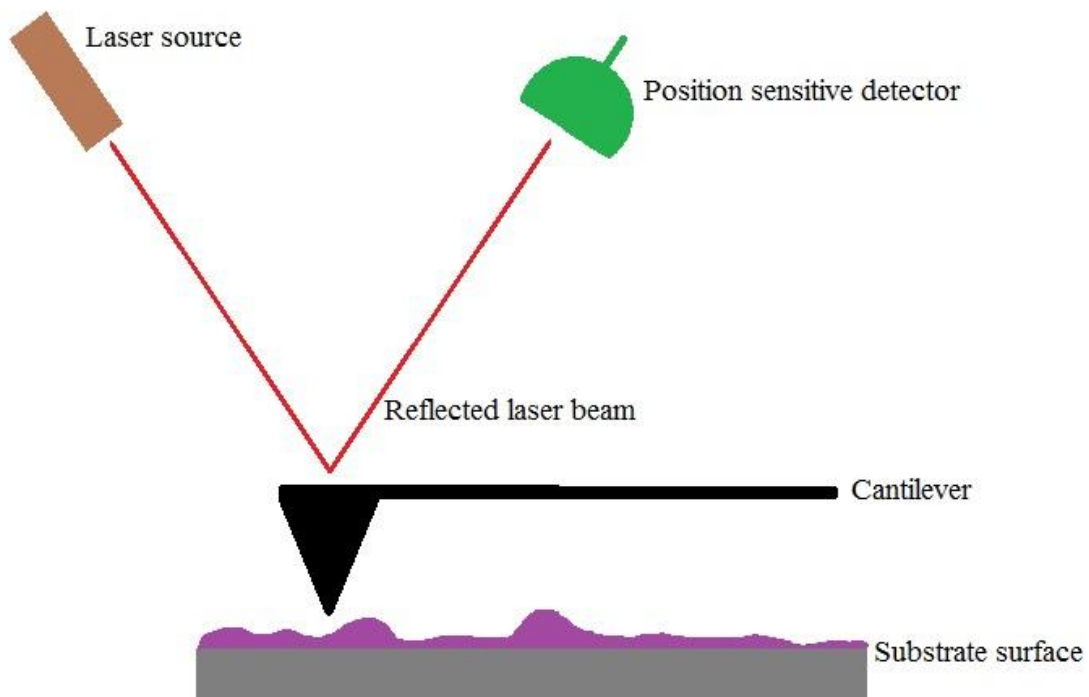


Figure 14: Scheme of an AFM

AFM can be operated in a variety of ways, such as contact mode, tapping mode, force spectroscopy and so on. Only the contact mode was used in this work to create the images shown. This mode is quite easily described: The tip of the cantilever is being moved over the substrate surface and therefore generates a topography image of the sample surface. In order to measure soft samples, which would deform under the force of the tip, the microscope keeps constant force between the tip and the surface by moving the cantilever following sample topography. This change in cantilever height can then be measured by the deflection of a laser beam reflected off the backside of the cantilever and is translated by software into a topographic image.

2.9. Alternative detection methods for bacteria

S. epidermidis is known since 1884, as was already mentioned in section [2.5], and was distinguished from other bacteria strains by the color of the bacterial colonies [24]. The color alone, of course, is not sufficient for distinguishing different bacteria. Therefore other detection methods have been established during the last centuries. The methods used today are mostly based on the polymerase chain reaction (PCR), enabling the analyst to detect different strains of *S. epidermidis* amongst other bacteria [34] [35]. This method, however, is not suited for in-situ measurements, since it requires extraction, multiplication, amplification and detection of gene sequences or the whole DNA of the organisms.

Another detection method, established by Xiang et al, uses different oxygen consumption of bacteria strains for their differentiation by differential pulse voltammetry [36]. Even though the method can be automated, it still requires cultivating the organisms as well as stationary measurement conditions and biofilm formation on the electrode surface, hence making it poorly suited for continuous monitoring of water supplies.

Golabi et al developed a detection method for different bacteria using asymmetric polypyrrole, a polymer with diverse physicochemical properties and different surface charges introduced by oxidation and counter ions. As the different bacterial strains have different surface chemistry, they adhere differently to the polymer surface. After the cells are bound to the polymer, they are fluorescent labeled and evaluated using optical microscopy [37]. This method is quite cheap and as fast as adhesion of the bacteria to the polymer, but is not suited for monitoring in flow systems, because it requires stationary conditions for adhesion.

Hence it can be concluded that currently no suitable method exists to detect *S. epidermidis* in situ in flow systems, like urban water supplies. It is therefore interesting to investigate the possibility of using MIP-QCM as sensor for the detection of the analyte in question, being a rapid, sensitive and selective method for the task in hand.

3. EXPERIMENTAL

3.1. Materials

All chemicals were purchased from VWR International GmbH. *Staphylococcus epidermidis* ATCC[®] 12228[™] was purchased from ATCC The Global Bioresource Center.

Optical microscope images were recorded using a Nikon Eclipse LV100 microscope.

AFM data was recorded using a Nanoscope VIII AFM by Bruker Metrology Corporation. Data was evaluated using the freeware “Gwyddion”, version 2.44, downloaded from www.gwyddion.net on 18.03.2016.

The frequencies of the QCMs after and before different coating steps were recorded using an Agilent 8712ET network analyzer and the data was evaluated using Microsoft Office Excel.

Oscillator measurements with QCM were carried out using a self-made measuring cell, which will be described in detail in section [3.5.5], and evaluated using an Agilent 53220A frequency counter.

3.2. Experimental procedures

3.2.1. Bacteria cultivation

The *Staphylococcus epidermidis* ATCC[®] 12228[™] strain used in this work was cultivated according to manufacturer’s protocol. Therefore the cells were grown in a plastic tube, kept at 37 °C in a water bath, in approximately 30 ml nutrient solution.

The nutrient solution used for the bacteria was made by mixing the following components in their relative weight percentage as stated below:

1 % Protease Peptone

0.5 % NaCl

0.1 % Glucose

100 % distilled water

For example:

2 g Protease Peptone

2 g Yeast extracts

1 g NaCl

0.2 g Glucose

200 ml distilled water

This mixture was heated to 100 °C to ensure complete dissolution of the components. After cooling the solution to room temperature aliquots of approximately 30 ml were frozen for storage or used to cultivate bacteria.

While digesting glucose, *S. epidermidis* produces waste products, which need to be washed away to ensure good growth environment for the bacteria. To do so the nutrient solution is separated from the bacteria by centrifugation at 1300 rpm for 5 minutes. Afterwards the pellet containing the cells is resuspended in distilled water and centrifuged again at the same conditions. The new pellet is then suspended in approximately 30 ml nutrient solution and kept at 37 °C. Bacteria were washed every other day.

3.2.2. Device manufacturing and characterization

A silkscreen method was used in order to deposit gold electrodes on the quartz wafers.

In a first step a piece of silk was fixed onto an iron frame with glue and overlaid with photo-sensitive dye (Azocol Poly-Plus S by KIWO). Using a stencil comprising the electrode structure and a UV lamp, the photo-sensitive dye hardened in the illuminated area. Afterwards the silkscreen was washed with water and dried at room temperature to remove the photo lacquer from non-exposed parts and thus reveal electrode geometry.

The silkscreen was then used to coat the quartz wafers with a brilliant gold paste containing gold colloid (GGP 2093 12%, purchased from the company Heraeus) and osmium tetroxide by placing the wafer on top of a Teflon holder. The silkscreen was then fixed on top of the wafer using holes in the iron frame. Gold paste was then deposited onto the silkscreen leaving only the electrode structure on top of the wafers. Afterwards the quartz substrates were heated to 400 °C for 3 hours to ensure the evaporation of linseed base oil, which left plain gold electrodes on the surface of the quartz wafers.

QCM measurements were carried out with a self-made measurement system, which consists of the measuring cell (Figure 15), an oscillator circuit, the frequency counter, connected to a computer with evaluation software, and a power supply, as can be seen in Figure 16.



Figure 15: Measuring cell consisting of (from left to right):

Cell containing a QCM, top with inlet and outlet tube and lid with 4 screws

QCM sensors are placed in the measuring cell connecting the bottom-side electrodes to the contacts on the left-hand and right-hand side of the cell, respectively. Afterwards the top is pressed firmly into the measuring cell and fixed with the lid and its screws. The cell contains a volume of about 200 μl on top of the QCM, which has to be filled with matrix solution before starting a measurement. In this thesis the matrix solution was distilled water. No liquid should flow underneath the QCM as this leads to erratic signals.

Measurements were always carried out using the following parameters: Stationary liquid, 12.4 V and 0.06 A on the power supply, 2 sec time interval for data recording.

The filled measuring cell is then connected to the oscillator circuit and the power supply, frequency counter and personal computer are switched on. Afterwards the measurement can be started. The liquid inside the measuring cell is exchanged by means of 200 μl Gilson pipettes.

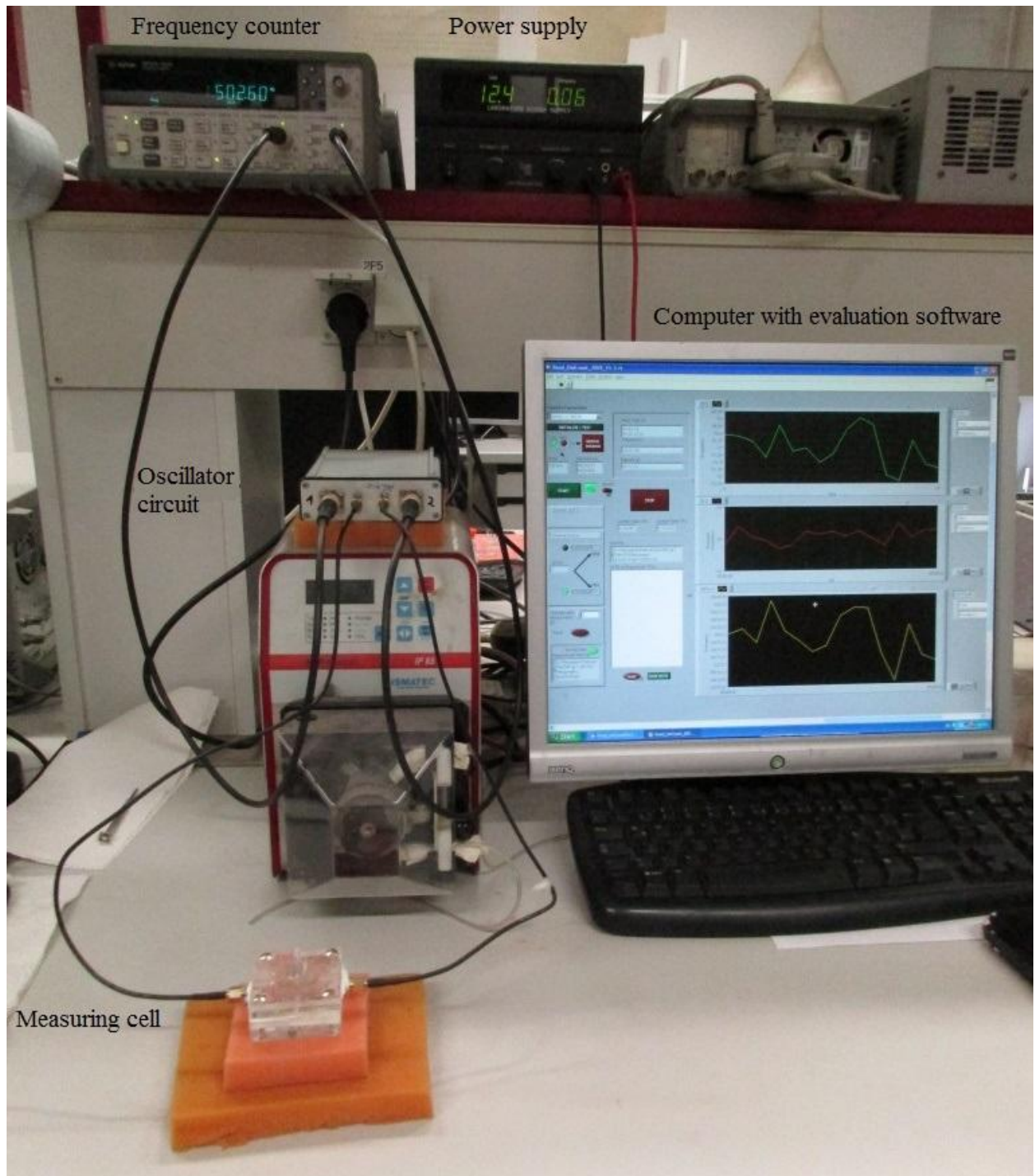


Figure 16: Measuring system

3.2.3. Imprinting protocols

All experiments were carried out at room temperature (~23 °C) and at atmospheric pressure.

In order to imprint templates into polymer thin films, the pre-polymer has to be coated onto the substrate, which can be realized by a variety of ways. In this work spin coating was used. In order to coat the pre-polymerized solution onto the substrate, a certain amount of liquid (in between 10 and 40 µl, depending on the polymer and required layer thickness) was placed on top of it. Then the substrate was rotated at a high speed (500 to 3000 rpm, again depending on polymer and required layer thickness). This spreads the solution onto the substrate during solvent evaporation, leading to very uniform and thin polymer layers that can be highly reproducibly generated.

Two imprinting methods, the stamp and the sedimentation imprint, have been tested for their suitability of imprinting the bacteria into the polymer: For both methods approximately 10 ml *S. epidermidis* in nutrient solution are centrifuged at 1300 rpm. The pellet is resuspended in 3.5 ml distilled water. This bacteria suspension is then used for imprints on QCMs and contains about 2.0×10^8 cells / ml. For imprinting on glass slides, one drop of Grams reagent is added to the solution, briefly shaken and centrifuged again at the same conditions. The colored bacteria are then dissolved in 3.5 ml distilled water to obtain the same concentration as before.

For stamp imprinting one drop (stained) bacteria suspension is placed on top of a polydimethylsiloxan (PDMS) stamp of 1 * 1 cm size and left to sediment for 30 minutes. After this time the stamp is rotated slowly on a spin coater at 800 rpm to remove excess solvent. Then 10 to 40 µl polymer solutions (depending on polymer and required layer thickness) are pipetted on top of the substrate (glass slide, QCM) and shortly spin coated at 500 to 3000 rpm. Immediately afterwards the stamp is placed on top of the substrate and pressed into the polymer overnight, to ensure complete hardening of the polymer.

For sedimentation imprinting the polymer is coated onto the substrate as before followed by placing a drop of (stained) bacteria solution as mentioned above on top of the polymer. A PDMS slide of 1 * 1 cm size is then used to press this drop into the polymer and left hardening overnight.

3.3. Stability study of frozen bacteria suspension

To investigate the stability of stained bacteria, 20 ml solution was separated into 7 aliquots of 2 ml each and stored at -20 °C for several days. The remaining solution was used otherwise. Stability of the respective bacteria was assessed by determining viability of frozen samples in light microscopy. After thawing the aliquot at room temperature 3 drops of 20 µl suspension were placed separately from each other onto a common microscopic glass slide. These drops were then investigated using the optical microscope. At least 2 images of every drop at 1000 times magnification were recorded to ensure statistical significance. In order to create a reference point, one bacteria sample was observed immediately after staining. Those cells were clearly alive, moving around randomly and most cells were separated from each other. These attributes correspond to the vitality of *S. epidermidis*, because dead cells do not move on their own and agglomerate. All frozen samples were treated the same way before being measured: they were thawed at room temperature, shaken briefly and analyzed immediately afterwards. Samples that showed vivid behavior were considered stable and images of all samples were taken. Samples for the following time spans were prepared and assessed: 0 days (reference point), 1 day, 2 days, 5 days, 7 days, 8 days and 14 days. Detailed results and a discussion of those will be shown in section [4.1].

In a second study 20 ml unstained bacteria solution was again separated into 7 aliquots of 2 ml volume each and stored at -20 °C for several days. These samples were tested for their stability by measuring them with a QCM as described in section [3.2.2] and the signal intensity was compared to that of a 0.3 mg/ml standard solution of *S. epidermidis*, which was always freshly prepared before measurements.

3.4. Polymer screening by QCM measurements

Analytes such as *S. epidermidis* usually show inherent affinity to different material surfaces. Such preferences can cause improved results when imprinting the cells into the polymer [38]. In order to investigate the affinities of the bacteria to different polymers, QCMs were coated with different non-imprinted polymers. The second electrode remained uncoated and served as a reference. Measuring these quartzes in water and adding an aqueous solution of *S. epidermidis* lead to a frequency drop on both electrodes, thus generating a clearly visible signal on the frequency counter. If the response of the NIP was higher than that on the pure gold electrode, the bacteria were considered to be naturally affine to the corresponding polymer. For each polymer

two QCMs were prepared to ensure repeatability of the results. Table 1 shows the polymers tested and their respective syntheses.

The results of this approach are shown and discussed in detail in section [4.2].

Polystyrene (PS)	
Styrene	120 μ l
Divinylbenzole	180 μ l
AIBN	6.5 mg
10 min 70 °C water bath	
Dilute with 600 μ l THF	

Polymethacrylic acid (PA2)	
Methacrylic acid	20 μ l
Ethyleneglycoldimethacrylate	29 μ l
DMF	500 μ l
Dichlormethane	240 μ l
AIBN	5.8 mg
1.5 h 55 °C water bath	

Polyurethane (PUeq)	
PG	31.2 mg
BPA	118.0 mg
DPDI	203.6 mg
THF	200 μ l
15 min ultra sonification	
Add 100 μ l solution to 880 μ l THF	
DABCO	20.7 mg in 1 ml THF
Add 20 μ l DABCO solution	
10 min 70 °C water bath	
Dilute 200 μ l polymer solution with 800 μ l THF	

Polyvinylpyrrolidone (PV)	
Vinyl-2-Pyrrolidone	19 μ l
EGDMA	29 μ l
DMF	500 μ l
Dichlormethane	240 μ l
AIBN	5.4 mg
2.33 h 55 °C water bath	

Polyacrylamide (PA)	
Sodiumperoxidisulfate	305.4 mg
Dissolve in 1 ml H ₂ O -> SL1	
DHEBA	17.0 mg
MAA	8 μ l
Dilute with 1000 μ l H ₂ O	
15 min ultra sonification	
LS1	17 μ l
10-15 min 55 °C in water bath	

Table 1: Polymers used for polymer screening

3.5. Polyurethane

3.5.1. First polyurethane QCM measurements

For first tests 5 QCMs were coated with polyurethane based on the recipe in Table 1 and imprinted with *S. epidermidis*. The polymer was prepared as follows: Phloroglucinol, bisphenol A and DPDI were weighed in into a 1 ml Eppendorf-tube according to Table 1 and mixed with 200 µl THF. This mixture was placed into an ultrasonic bath for 15 minutes at room temperature to ensure complete dissolution of all components. Afterwards polymerization was carried out by placing the tube in a water bath at 70 °C for 30 minutes. After polymerization, 50 µl of this solution were diluted with 950 µl THF in another Eppendorf-tube and used for spin coating. In order to ensure coating on only one electrode pair, a piece of adhesive foil was equipped with two holes each the size of the respective electrode. This foil was affixed to the QCM in a way which leaves the electrodes uncovered. The quartz was then placed on top of the spin coater and 40 µl polymer solution were pipetted onto the QCM. The device was then spun at approximately 2000 rpm for roughly 2 seconds and removed from the coater. For these QCMs the stamp imprint method, as described in [3.2.3], was used. After hardening the polymer, washing the quartzes with distilled water and analyzing them on the network analyzer, the QCMs could be used for measuring in the oscillator circuit (see section [4.3.1]).

3.5.2. Polyurethane screening on glass slides

In order to screen polyurethanes, glass slides were coated with different polyurethanes and then imprinted with *S. epidermidis*. Non-catalyzed polyurethane was produced as described in Table 1. To synthesize the catalyzed polymer 100 µl of the monomer solution were diluted with 880 µl THF after treatment in the ultrasonic bath and polymerization was initiated using 20 µl DABCO-solution (20 mg DABCO in 1 ml THF). This initiated solution was then heated to 70 °C in a water bath for 8 min. Then 200 µl of the resulting solution were diluted with 800 µl THF. This last dilution was then used for spin coating as described before. Table 2 gives the exact compositions of the polyurethane batches used in these experiments.

To investigate the effect of the imprinting method on the distribution of cells on to the glass slide, both imprinting techniques described in section [3.2.3] were used for all polymers tested.

The results of these experiments will be discussed in detail in section [4.3.2].

Used polymers					
Name	PG [mg]	BPA [mg]	DPDI [mg]	% excess	Excess group
PUeq	32	119	205	2	Isocyanate
PU10OH	33	133	200	9	Hydroxy
PU25OH	39	150	204	24	Hydroxy
PU50OH	46	180	202	49	Hydroxy
PU10CN	27	109	209	14	Isocyanate
PU5OH	32	126	201	5	Hydroxy

Table 2: Different polyurethane compositions used

3.5.3. Determining the layer heights of PUeq

In order to achieve repeatable layer thicknesses during QCM coating, all layers were deposited with the spin coater Spincoat G3P-8 by SCS with the possibility to choose exact time values for acceleration, rotation and slowing down as well as exact rpm for rotation speed. To determine which time values and parameters have to be chosen to create the required layer thicknesses (as will be discussed in section [4.3.3]), 29 quartzes were coated using different settings. Time values were set to 2 s for acceleration, 5 s for rotation and 0 s for slowing down and found to be the best values for the required layer thicknesses. Then the rotation speed was changed in 500 rpm steps in between 500 and 3000 rpm. All tested parameter combinations are shown in Table 3. The polymer compositions used are shown in Table 4 and are as close to PUeq as possible.

Tested parameter combinations			
Acceleration [s]	Rotation time [s]	Slowing down [s]	Speed [rpm]
2	5	0	500
2	5	0	1000
2	5	0	1500
2	5	0	2000
2	5	0	2500
2	5	0	3000

Table 3: Combinations of tested parameters

Each polymer composition was tested on at least 6 quartzes to ensure statistical relevance. Furthermore for each rotation speed tested at least 2 quartzes were coated in the same manner. After hardening the QCMs were analyzed on the network analyzer and the change in frequency before and after coating was used to determine layer thickness using the Sauerbrey-equation. The calculation has been given in detail in section [2.2.4].

Because the first experiments revealed insufficient layer thicknesses, the amount of polymer solution was changed (see Table 4). The last polymer in the tables refers to a composition for which final dilution is based on mixing 300 μ l pre-polymerized solution with only 700 μ l THF. The polyurethane used was catalyzed using DABCO solution as described before (see section [3.5.2]). Results will be discussed in detail in section [4.3.3].

Used polymers						
Name	QCMs	PG [mg]	BPA [mg]	DPDI [mg]	% excess	Excess group
PUeq 20 μ l	R37-R48	32	118	204	2	Isocyanate
PUeq 30 μ l	R49-R54	31	118	201	1	Isocyanate
PUeq 40 μ l	R55-R60	31	118	198	1	Hydroxyl
PUeq 30 μ l 7:3	R61-R66	31	118	205	3	Isocyanate

Table 4: Polyurethane compositions used for layer thickness determination

3.5.4. Template removal from PUeq

In order to generate cavities in the surface of the polymer layer, the imprinted bacteria need to be removed after hardening of the polymer. The first step of the experiments was to imprint colored bacteria into the polymer on glass slides, using a layer thickness between 200 and 300 nm. The glass slides were then washed with distilled water in a Petri dish and stirred magnetically for 1 hour. Some other solutions were also tested for their washing effects on the bacteria, including 0.5 % hypotonic NaCl solution (as for the nutrient solution of the bacteria), AgNO₃ solutions with different AgNO₃ concentrations (according to Yang et al [39]) and a washing solution consisting of NaOH 0.2 mol/l and 1 % SDS (used in different dilutions, from 1:20 to 1:1). The success or failure of these methods was controlled by using optical microscopy. After the final washing step AFM measurements were carried out to prove that the structures visible in light microscopy were actually cells and not cavities. Results of the removal studies are given and discussed in section [4.3.4].

3.5.5. QCM measurements

Even though it was not possible to remove all imprinted cells from the polymer (see [3.5.4]), first tests showed promising results for QCM measurements (see [3.5.1]). Therefore more quartz sensors were coated with PUeq with layer thicknesses between 200 and 300 nm and imprinted with *S. epidermidis* on the channel with lower resonance frequency. After washing the imprinted QCMs with water for 1 hour, to remove dust and non-polymerized monomers, the sensors were characterized in distilled water using the QCM measurement system described in section [3.2.2].

For determining sensitivity of the QCMs an aqueous solution containing $2.5 \cdot 10^8$ cells / ml *S. epidermidis* was diluted 1:2, 1:3 and 1:5. Each dilution was assessed by pipetting 200 μ l solution into the measuring cell.

In order to test the sensors for selectivity, solutions of *B. cereus* (concentration: $1.8 \cdot 10^8$ cells / ml) and *E. coli* (concentration: $9.5 \cdot 10^7$ cells / ml) were prepared. These solutions were assessed by pipetting 200 μ l solution into the measuring cell again.

Results and discussions of those will be given in section [4.3.5].

3.6. Polymethacrylic acid

3.6.1. Determining the layer heights of PA2THF

The experiments for layer thickness determination for polymethacrylic acid were carried out in the same way as for polyurethane (see section [3.5.3]). However, in contrast to polyurethane, composition of PA2THF was not changed. The general recipe for polymethacrylic acid, according to Ji et al [40] was as follows: First, 2.5 mg AIBN were weighed in and mixed with 20 µl methacrylic acid and 29 µl EGDMA. This mixture was then dissolved in 740 µl THF and pre-polymerized at 60 °C in a water bath for 1.5 hours. The resulting liquid was then used for coating experiments.

The first layer thickness experiments resulted in too high layers, even at 3000 rpm and when using only 10 µl polymer solution. Therefore more diluted samples were prepared by dissolving the reagents in 800 µl THF instead of 740 µl. The results of these experiments will be discussed in detail in section [4.4.1].

3.6.2. Template removal from PA2THF

The same washing procedures as for polyurethane were carried out for polymethacrylic acid, detailed descriptions of the used solutions can be found in section [3.5.4]. AFM and light microscopy images have been recorded for the washed glass slides in order to investigate the success of the removal, as will be discussed in section [4.4.2].

3.6.3. APTES stamp imprint

In order to create QCMs using stamp imprinting, suitable stamps had to be produced in a first step. To create the stamps using a slightly amended recipe from Hu et al [41], glass slides were cut into small squares of about 0.5 * 0.5 cm size and cleaned using ethanol and acetone. Afterwards one surface of the glass slides was activated by treating with oxygen plasma for 30 to 40 s using a plasma discharger. This activation generates free hydroxyl groups on the surface of the glass slides, enabling the binding of (3-aminopropyl) triethoxysilane (APTES) onto the substrates. Binding was carried out by immersing the activated slides in a solution of 1 % APTES in EtOH of 96 % purity for 2 h. Afterwards the stamps were shortly washed in distilled water. Then, a concentrated solution of *S. epidermidis* was placed on top of the activated APTES surface. After 10 min the bacteria solution was removed and the stamps were washed in distilled water for 1 h in order to remove unbound cells and dried overnight at room temperature.

The success of the immobilization was controlled using optical microscopy as well as AFM, which will be shown in section [4.4.3].

The stamps were then pressed into freshly coated polymer layers on QCMs as described in section [3.2.3]. After hardening for 2 days the stamps were removed from the QCMs. The quartzes were washed in water for 1 h and after drying and characterizing with the network analyzer inserted into the measuring cell or the AFM.

3.6.4. QCM measurements

The first step to create working QCMs using PA2THF was to coat the electrodes of the quartz crystal with the polymer under conditions that lead to ideal layer thicknesses. To do so 5 μ l of pre-polymerized PA2THF solution was deposited onto each of the two electrodes, which were masked using adhesive foil. Afterwards the polymer was spin coated using 2 seconds for ramp time, 5 seconds rotation time, 0 seconds dwell time and 3000 rpm rotation speed. Then the MIP electrode was sedimentation imprinted using 5 μ l concentrated *S. epidermidis* solution and a piece of PDMS to press the cells firmly into the polymer. The NIP was imprinted using only a piece of PDMS. After two days hardening the PDMS was removed and the resonant frequencies of the QCMs were recorded, the sensors washed for 1 hour in distilled water, dried at room temperature and the frequencies recorded again. Afterwards the QCMs could be measured using the self-made measuring cells.

To test the sensors for linearity and selectivity a dilution series of a concentrated *S. epidermidis* solution was created and measured against a concentrated *B. cereus* solution.

Furthermore the sensor characteristics of QCM sensors obtained by this protocol have been evaluated as discussed in section [4.4.5].

4. RESULTS AND DISCUSSION

4.1. Stability study of frozen bacteria solution

Aqueous solutions of *S. epidermidis* were the major sample materials used in this thesis. Therefore it was necessary to assess stability of the frozen bacteria solutions as described in section [3.3]. Microscope images were taken after 0, 1, 2, 5, 7, 8, and 14 days storage at -20 °C, respectively. Images from each day, except day 8, are shown in Figure 17. The solutions were stained in order to alleviate the task.

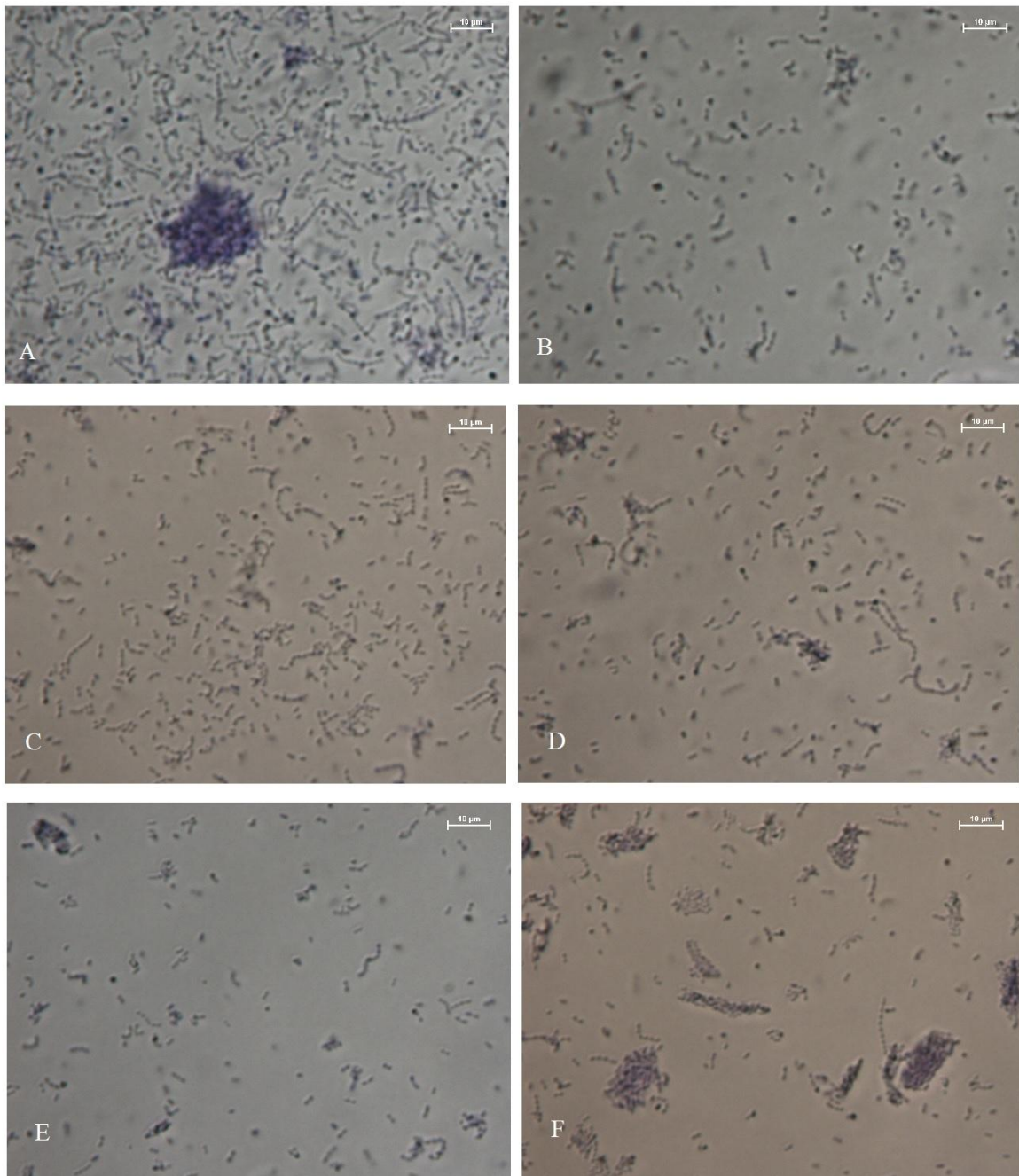


Figure 17: 1000 times magnified aliquot pictures after A: 0 days; B: 1 day; C: 2days; D: 5 days; E: 7 days; F: 14 days

It can clearly be seen that small cell agglomerations increase with increasing storage time. Agglomeration occurs at different conditions, one being the increasing number of dead cells. As more and more cells die, they attach to each other in a last attempt of survival, which may lead to the conclusion, that the frozen bacteria are not stable for a long period of time. But the mechanism may also occur as a defense strategy against osmotic pressure, as has been described previously [3], and may therefore just indicate the presence of osmotic stress for the cells. As the *S. epidermidis* solution consists of cells diluted in distilled water, the organisms are constantly under osmotic stress and therefore agglomerate continuously. Due to the different possible mechanisms the number of agglomerates should not be treated as indication for stability, which is why the vitality and movement of the cells was taken as stability parameter. Motion, of course, cannot be captured in an image, but nevertheless it could be seen under the microscope and it was possible to see large numbers of vividly moving *S. epidermidis* until the last day of the stability study.

Due to the observed vitality of the cells as well as the exceptionally high number of agglomerates on day 14 of the stability study, frozen *S. epidermidis* solutions were considered stable for at least 7 days when stored at -20 °C.

In the second part of the stability study the frozen aliquots were analyzed using QCMs, namely QCM number 42 and number 44. For these experiments the solutions were left unstained, as the staining agent could also dye the measuring cell and should not have any influence on the stability. As the QCM signal depends on different parameters including lab temperature, humidity or interfering electromagnetic signals, a freshly prepared reference solution with a concentration of 0.3 mg/ml was assessed in parallel to the aliquots and the signal ratios of sample and reference solution were evaluated. Figure 18 shows a typical stability study measurement, carried out with QCM #44 on day 3.

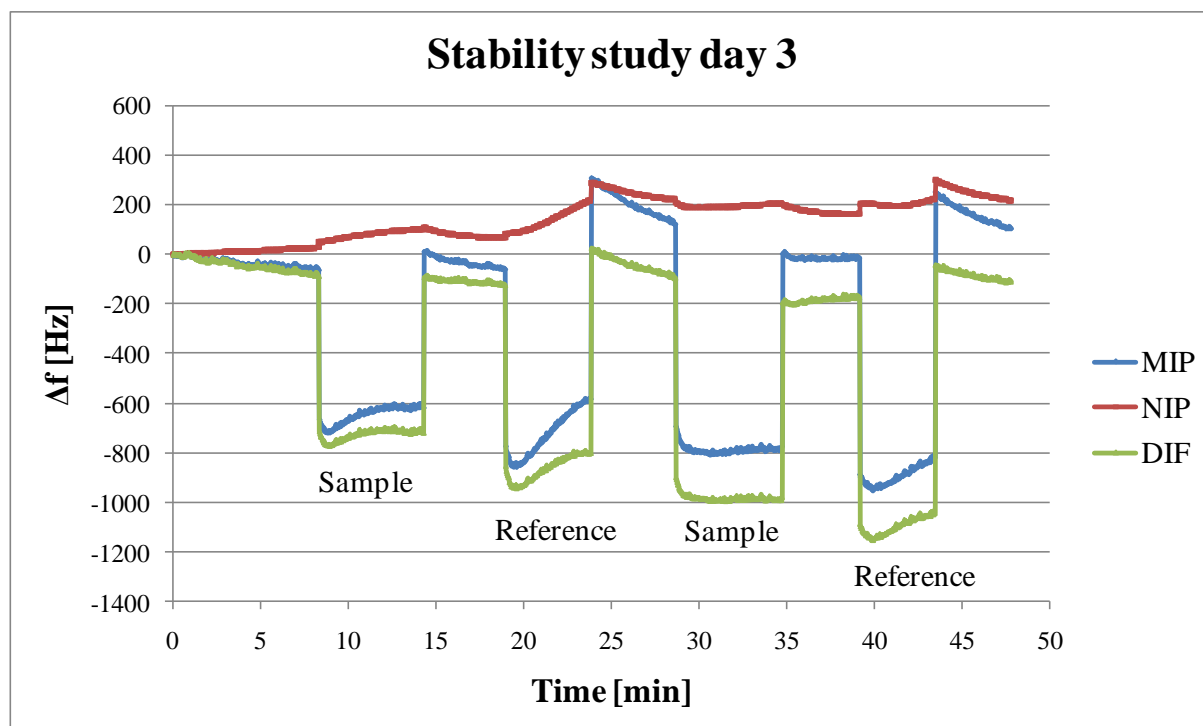


Figure 18: Stability study measurement for day 3

The red line in the graph indicates the frequency of the non-imprinted electrode, the reference channel, the blue line the signals of the molecular imprinted electrode, the sensitive channel. The green line is the difference of the MIP and the NIP (MIP - NIP) and therefore most interesting, as it represents the signal of the analyte corrected by environmental effects and signals created by side effects such as viscosity.

During each day of the stability study sensor response curves similar to the one above were recorded, the ratios between sample and reference calculated, and evaluated, as shown in Table 5. The ratios were calculated by dividing reference by sample.

Day No	Compared conc.	Ratio MIPs	Ratio DIFs
0	0.3 mg/ml	0.47	0.60
1	0.3 mg/ml	0.69	0.91
3	0.3 mg/ml	0.71	0.83
8	0.3 mg/ml	0.85	0.96
10	0.3 mg/ml	0.59	0.53
14	0.3 mg/ml	0.64	0.79

Table 5: Results of the stability study measurements

If the bacteria solution would not be stable, the signal of the sample solution should decrease with time, making the ratio reference / sample increase with time. At first glance this seems to be true, as the ratio increases from day 0 to day 1 and continuously stays on a higher value, but on day 10 the ratio drops down to a value almost as small as on the first day. If day 10 is considered an outlier, as an error in placing the QCM inside the measuring cell could have taken place, the values lead to the following graph Figure 19.

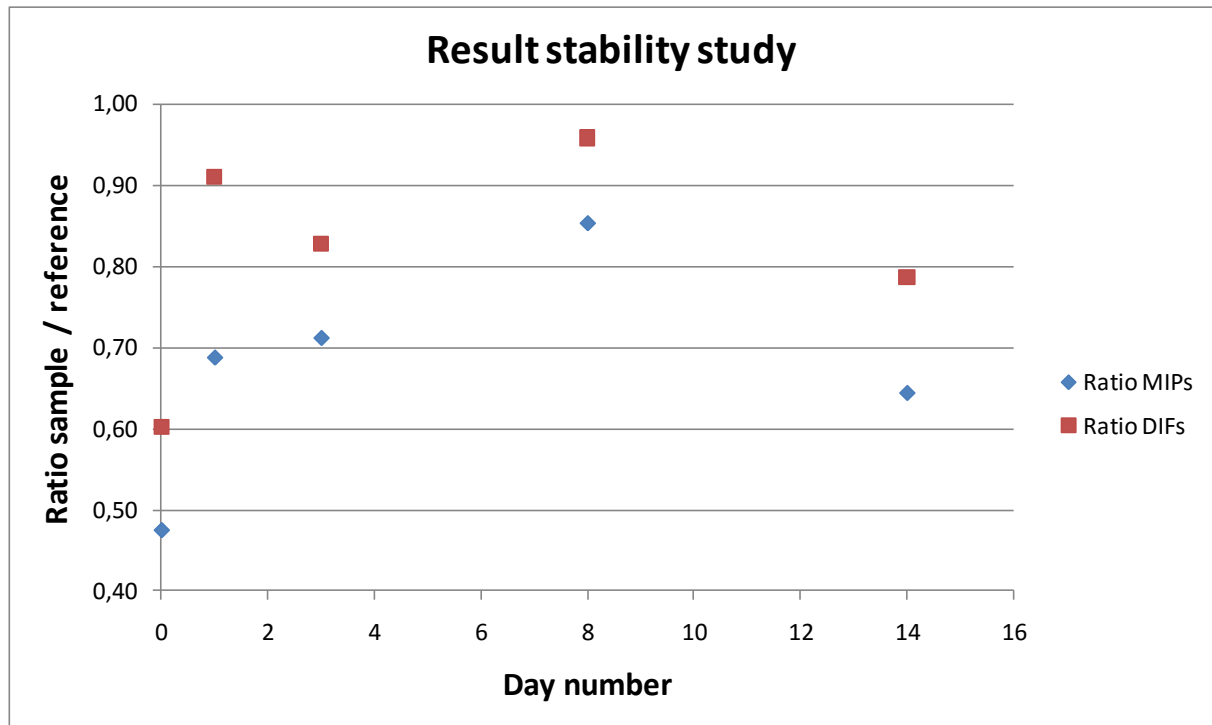


Figure 19: Ratios for MIP and the difference MIP - NIP against days; day 10 excluded

Results indicate that after one day storage at $-20\text{ }^{\circ}\text{C}$ a certain amount of cells dies, which leads to the increased ratio after day 0. After this first drop the signal obtained from the sample solution stabilizes and the ratio reaches a more or less constant value of about 0.87. Correlating the average ratio of all days except day 10 with the ratio of day 0 leads to a value of 0.69. This shows that after the first day 69 % of the cells stay alive throughout the duration of the stability study. It can therefore be concluded that after one day at $-20\text{ }^{\circ}\text{C}$ 21 % of the cells die. One possible explanation for this behavior could be that freezing leads to some sort of “lifeboat agglomeration” comprising of dead cells stabilizing the viable organisms [42]. Afterwards the surviving cells can stay alive for a long period of time, which would explain the constant ratio after day 1. This theory, however, would not explain the ratio drop on day 10, unless stability maximum is reached after 8 days. If many *S. epidermidis* cells would die in between day 8 and

day 10, the dead cells could sediment onto the electrode when measuring and lead to a high change in mass loading and therefore a higher signal.

However, the stability study measurements showed that the frozen *S. epidermidis* solution is, after a little drop on the first day, stable for at least 8 days, which correlates well with the result of the microscopic stability study.

4.2. Polymer screening by QCM measurements

As described in section [3.4], polyurethane (PU), polystyrene (PS), polymethacrylic acid (PA2), polyvinylpyrrolidone (PV) and polyacrylamide (PA) have been tested for natural affinity towards the target organisms. The polymer was coated onto one electrode; the other electrode was left as blank gold, as described previously. Measurements obtained are shown in Figure 20 and Figure 21, where the red line shows the polymer coated electrode and the yellowish one the blank gold electrode, respectively.

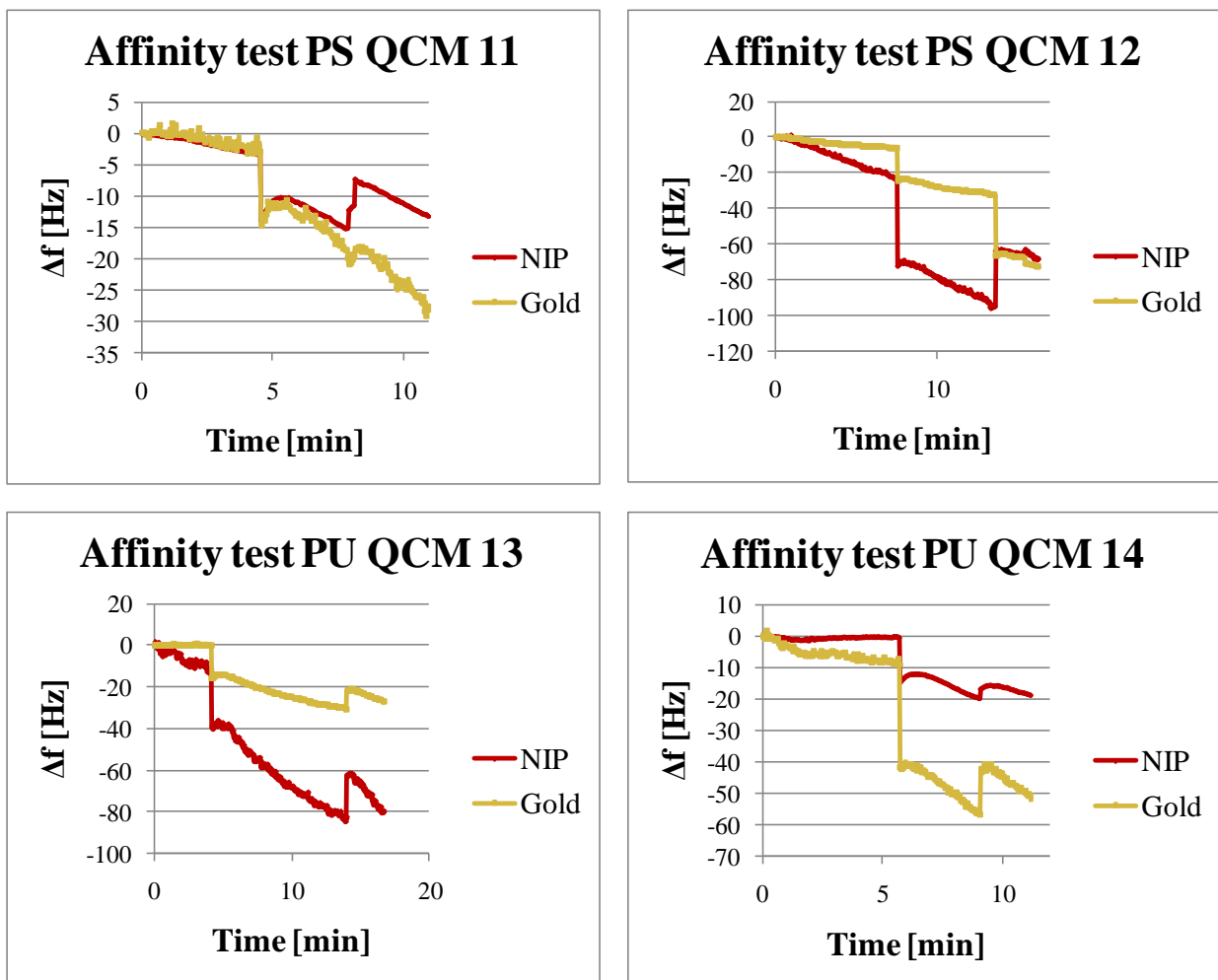


Figure 20: Affinity testing for polystyrene and polyurethane

It is clearly visible that *S. epidermidis* shows natural affinity to PU, as QCM 13 yielded a stronger signal on the NIP channel, than on the gold electrode. Signal intensity of about 20 Hz is the same for both QCM 13 and 14, even though the response of the gold electrode is 15 Hz higher for the second sensor. This may be due to electrode geometry, because the electrodes are always individually different from each other due to the production process described in section [3.2.2].

Affinity of PS to *S. epidermidis*, however, is lower than of PU, as only one of two QCM revealed a clear signal, even though the magnitude obtained was higher than for PU.

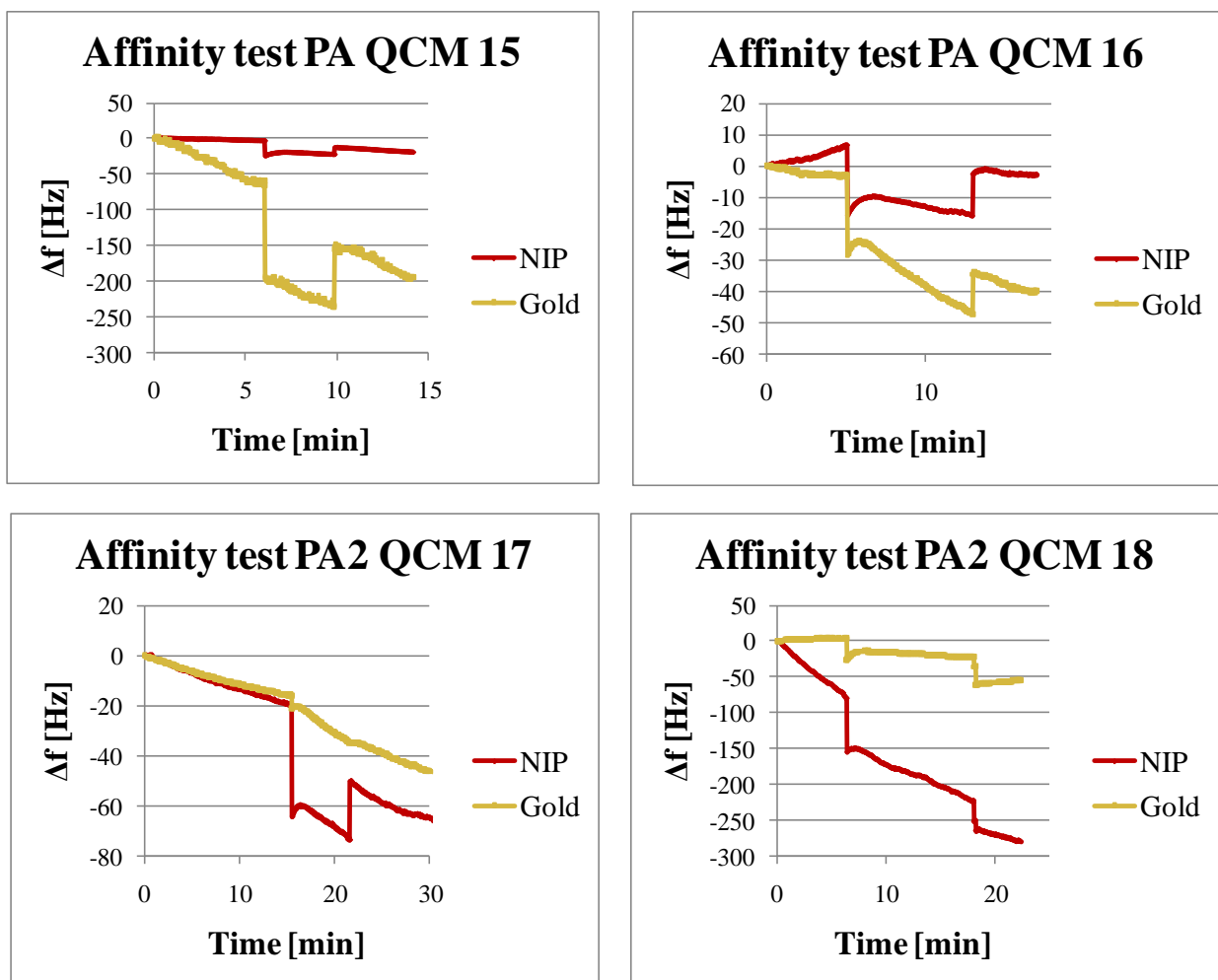


Figure 21: Affinity testing for polyacrylate and polymethacrylic acid

The target organism showed no natural affinity to PA, as can be seen in Figure 21, because the signal of the gold electrode was at least 10 Hz higher on QCM 16 and more than 100 Hz higher for QCM 15. For all other measurements the signal of the analyte was rather low, namely less than 20 Hz, which again indicates low affinity.

For PA2, polymethacrylic acid, the strongest affinity of all polymers could be observed. Both QCM 17 and 18 showed an intensive signal of more than 40 Hz, which was stronger than the signal of the gold electrode.

Polyurethane and polymethacrylic acid were therefore the two polymer systems that showed best natural affinity. As polyurethane had already been known to be useful for QCM imprinting experiments [22], it was decided to start the research for an *S. epidermidis* sensor with this polymer, as will be described in the following section.

4.3. Polyurethane

4.3.1. First polyurethane QCM measurements

Due to the natural affinity of *S. epidermidis* to polyurethane, as demonstrated in section [4.2], some first “quick and dirty” trials of QCM production were carried out, as described in section [3.5.1]. Ten QCMs were produced, four of which showed responses to a concentrated solution of *S. epidermidis* by decreasing in frequency. One sensor even showed selectivity against a reference solution of *E. coli*, a rod-shaped bacterium. The response pattern of the selective QCM is shown in Figure 22, representing the average response to *S. epidermidis*.

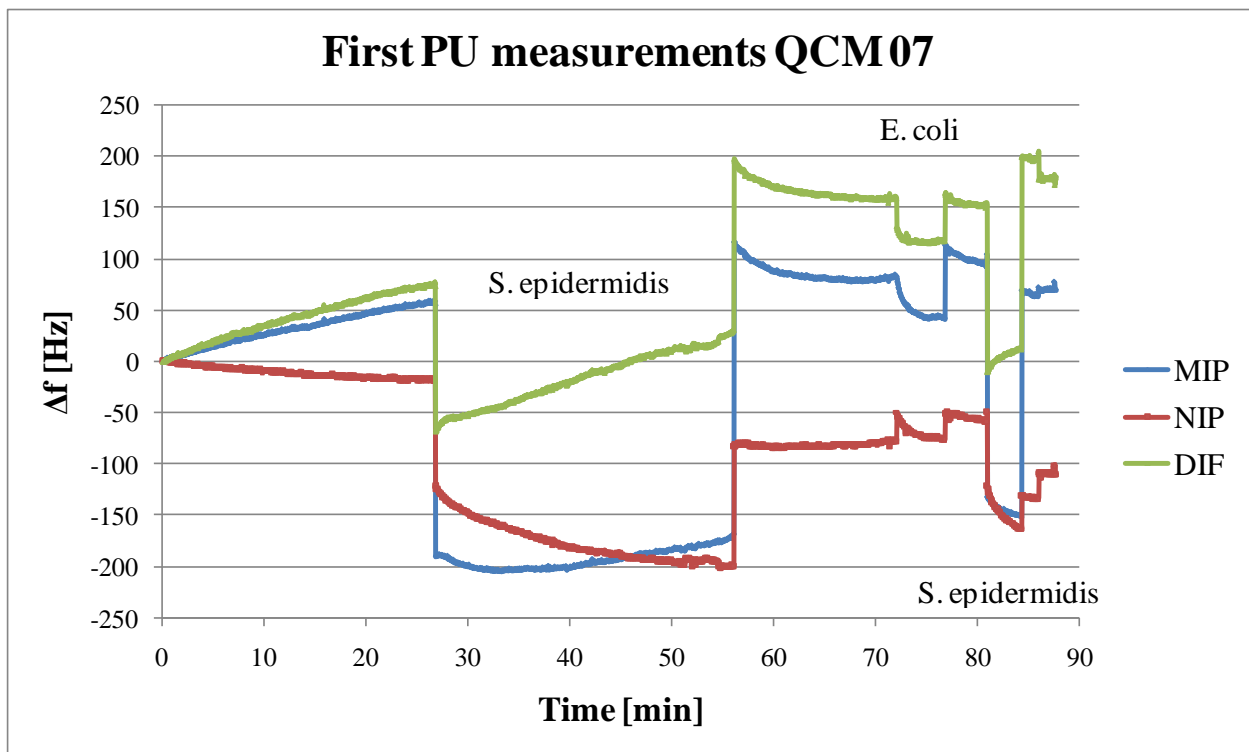


Figure 22: First QCM measurement of *S. epidermidis* using polyurethane

The first and the last signal result from the same analyte solution with a concentration of about $2.7 \cdot 10^8$ cells / ml; the second, very low signal represents a concentrated ($3.1 \cdot 10^8$ cells / ml) solution of *E. coli*. It is clearly visible that the QCM responded about 4 times stronger to the imprinted bacteria than to the reference organism. This result could be repeated on 4 out of 10 sensors, wherefore it was decided to start optimization experiments using polyurethane.

4.3.2. Polyurethane screening on glass slides

Polyurethane is synthesized from phloroglucinol, bisphenol A and diphenylmethane-4, 4'-diisocyanate (DPDI), three substances with different properties that contribute either OH- or OCN- groups to the polymer. Therefore the structure and properties of PU varies, depending on the relative amount of reactive groups and furthermore on the overall amount of monomers used. Such different properties may also influence quality of the imprint. Moreover, the polymer can be catalyzed using DABCO as a catalyst and again change its structure. Therefore it makes sense to screen different compositions of polyurethane, as described in section [3.5.2].

In order to do so the concentrations of phloroglucinol, bisphenol A and DPDI were varied. Furthermore catalyzed and non-catalyzed polyurethane were compared. Finally stamp and sedimentation imprinting method, described in section [2.4.2], were compared.

The optical microscope images of both systems shown in Figure 23 compares catalyzed and uncatalyzed PU after cell imprinting.

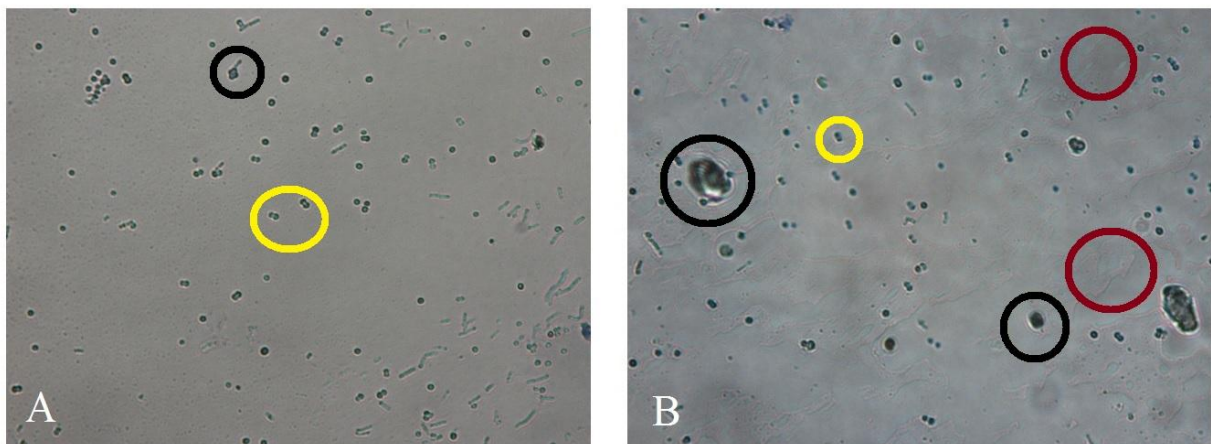


Figure 23: Comparison of A: catalyzed PU and B: not catalyzed PU; 1000 times magnification

It can easily be seen that the non-catalyzed polyurethane reveals higher roughness (red circles) compared to the catalyzed one, as well as some major impurities (black circles), that exceed the number of cells (yellow circles) in height and diameter. Furthermore when not using catalyst, the polymer becomes a random mixture of polyurethane and polyurea, whereas the catalyzed polymer consists of polyurethane mostly, as was described in previous work (see [43]). It was therefore concluded that using the catalyzed polyurethane should lead to superior results when creating a sensor for the detection of *S. epidermidis*.

During a second experiment the two imprinting techniques described in section [2.4.2] were compared for all polyurethane compositions, leading to approximately the same results. Figure 24 shows two exemplary microscope pictures with 1000 times magnification of catalyzed polyurethane imprinted via sedimentation imprinting and stamp imprinting, respectively.

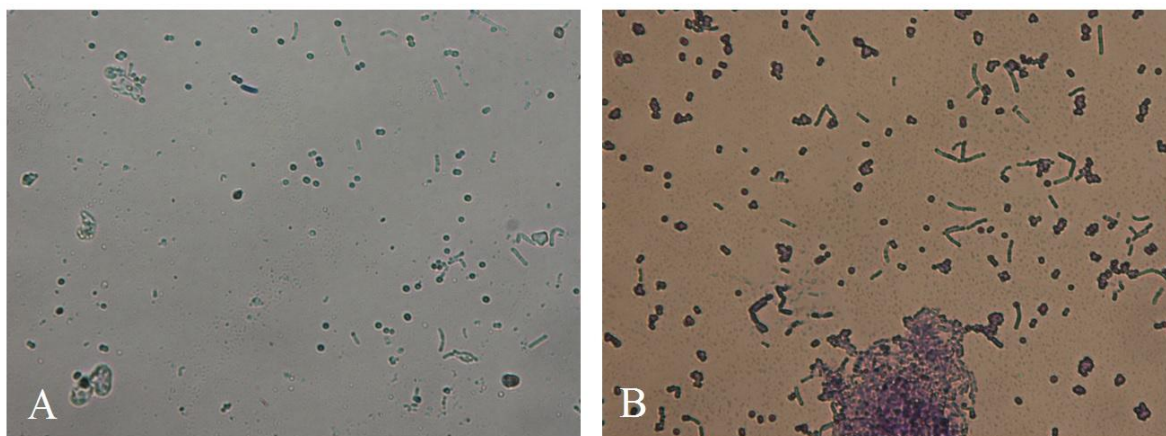


Figure 24: A: sedimentation imprint and B: stamp imprint using catalyzed polyurethane; 1000 times magnification

It can easily be seen that the stamp imprint (Figure 24 A) shows large agglomerations of *S. epidermidis*, which results from the long time the bacteria were left to self-assemble on top of the PDMS stamp. The aim of the work was to create a sensor for cells in solution, which means that the cells are most probably not agglomerated, as they move freely inside the solution. It was therefore concluded that the stamp imprinting technique is not suited for imprinting the analyte, as it would create cavities the size of agglomerates, not the size of single cells.

Finally, the six different polyurethane compositions described in Table 6 were tested for their suitability of imprinting *S. epidermidis*. “Description” in the table refers to the ratio of hydroxyl and isocyanate groups in the final polymer.

Used polymers			
Name	Description	% excess	Excess group
PUeq	OH = OCN	0	Isocyanate
PU10OH	OH = 1.1 * OCN	10	Hydroxy
PU25OH	OH = 1.25 * OCN	25	Hydroxy
PU50OH	OH = 1.5 * OCN	50	Hydroxy
PU10CN	OH = 0.9 * OCN	10	Isocyanate
PU5OH	OH = 1.05 * OCN	5	Hydroxy

Table 6: Used polymers for polyurethane screening.

Again, exemplary microscope images at 1000 times magnification of all polymer systems are shown (Figure 25). These exemplary pictures prove that the polyurethane composition with the approximately same amount of hydroxyl and cyanate groups is best suited for the imprinting experiments. The distribution of the cells in picture A is very homogenous, the cells are not agglomerated and there are more cells than on other polymer compositions. Picture B and F, the polyurethanes with 10 % more hydroxyl or 10 % more cyanate groups, showed agglomeration of the bacteria; this led to the impracticality of these compositions for imprinting. The other hydroxyl excess polymers showed too few imprinted cells.

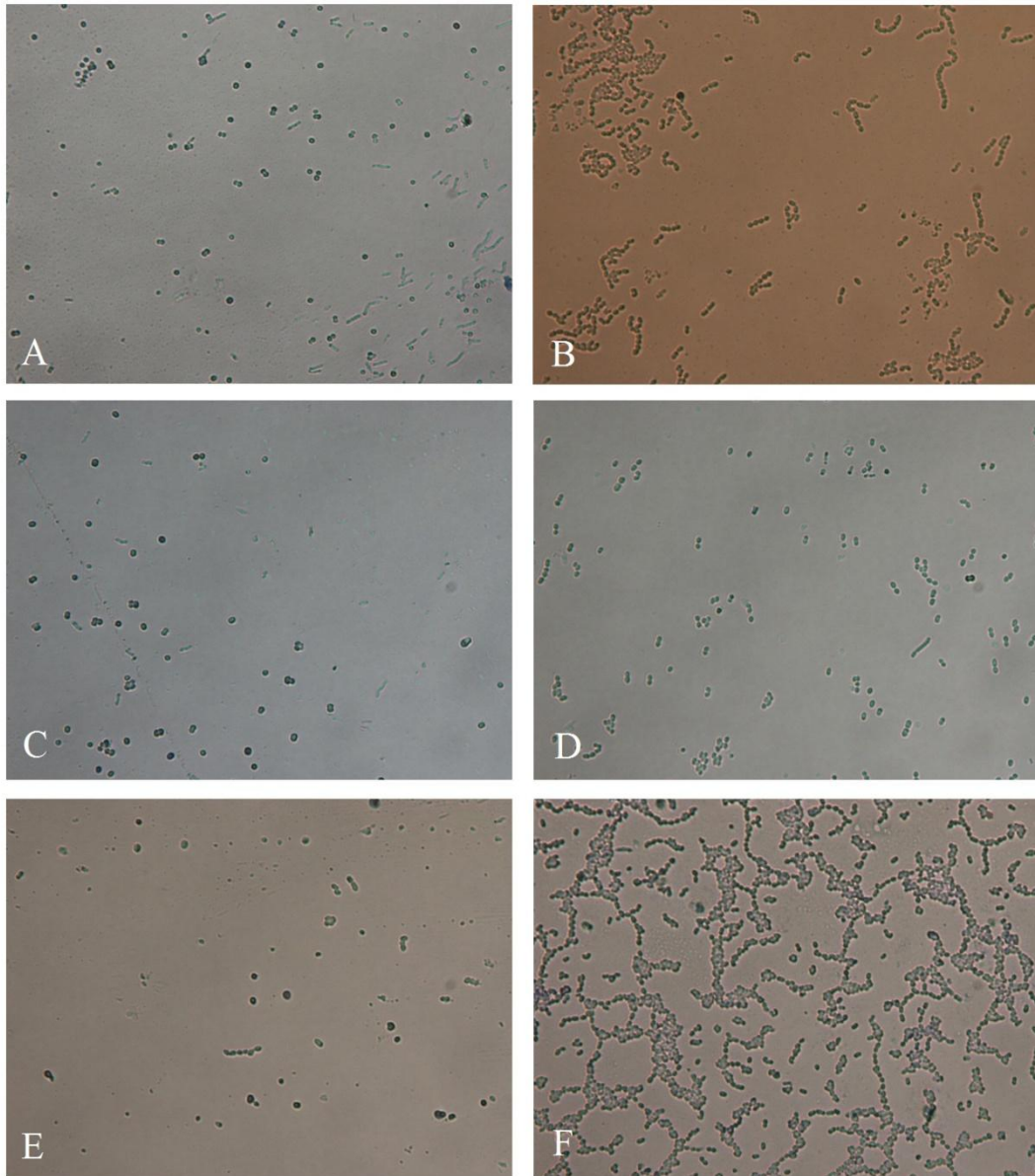


**Figure 25: Comparison of different polyurethane systems, 1000 times magnification.
A: PUeq; B: PU5OH; C: PU10OH; D: PU25OH; E: PU50OH; F: PU10CN**

All these experiments led to the conclusion that catalyzed polyurethane with an equal amount of functional groups and sedimentation imprinting method should be best suited for imprinting *S. epidermidis*.

4.3.3. Determining the layer heights of PUEq

Based on the optimal polymer, catalyzed polyurethane with an equal amount of OH and OCN groups, the next step comprised of determining layer thicknesses as described in section [3.5.3]. Layer thickness was calculated using the Sauerbrey equation as described in section [2.2.4] based on the frequency changes of QCM measured using the network analyzer. Figure 26 shows exemplary frequency measurements recorded with the network analyzer.

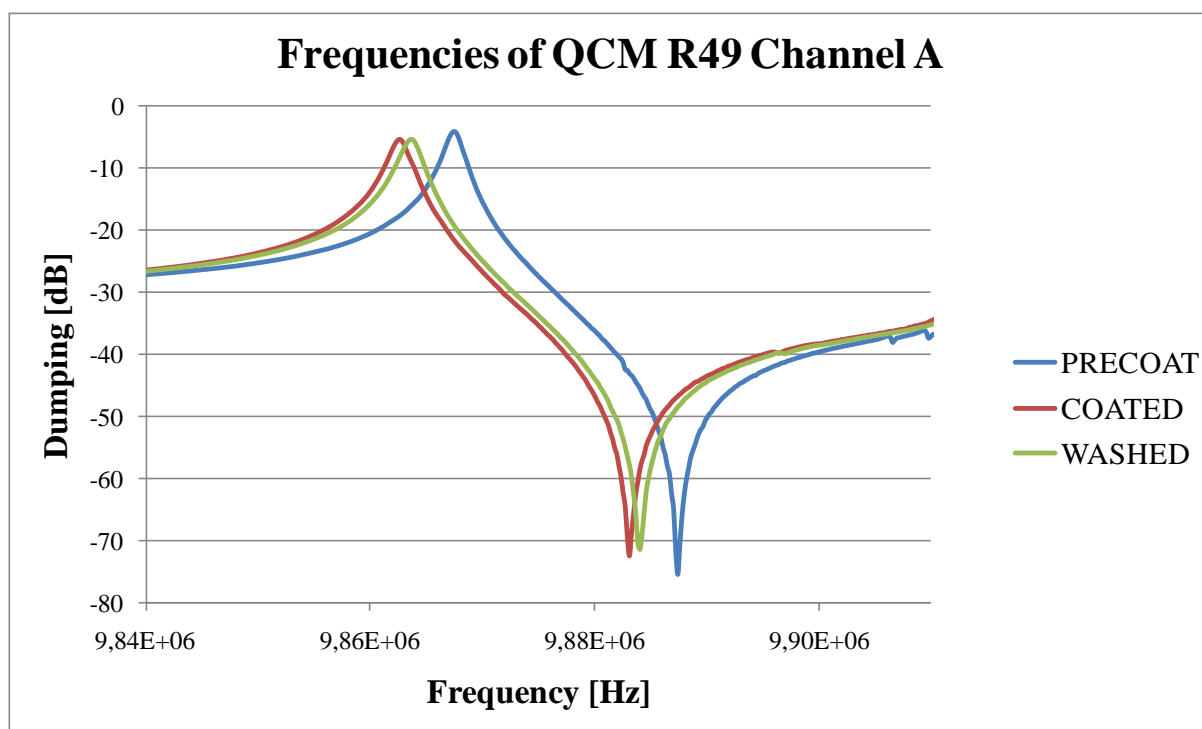


Figure 26: Network analyzer measurement of QCM R49 Channel A

The frequency used for calculation was always the one at the minimum damping, which is the value at the first maximum of the curve in Figure 26. Damping describes the loss of amplitude due to mass loading or defective electrodes. It is therefore necessary to reach lowest damping possible for each sensor, as high damping leads to erratic results. The blue line represents the measurements carried out on pure gold electrodes. The red line shows the frequency spectrum measured after spin coating, imprinting and hardening of the polymer, respectively. The green line represents the values after the coated QCM was washed in distilled water for one hour and dried again. The graph shows that the frequency (maximum of the first peak) decreases after coating as the mass loading on the electrode increases. After washing some dust and unpolymerized monomers are washed away from the polymer layer, wherefore the frequency increases again as the mass loading is slightly decreased.

The aim of the experiment was to determine the layer thickness of the final polymer layer as a function of the rotation speed and amount of polymer used. For that purpose the data of different polymers after polymerization and rinsing with water were compared. The desired layer thickness was 250 nm, because the bacteria are at least 500 nm in diameter. As the aim of this work is to create cavities on top of the polymer surface, layer height has to be less or equal half the minimum diameter of the analyte. The MIP should be thick enough to create cavities of suitable size, but small enough to not cover the cells in order to enable removal of the cells after imprinting. To ensure statistical significance, two QCMs, each carrying two electrodes, were used for each rotation speed and amount of polymer, hence leading to a total of 4 values for each rotation speed experiment. Figure 27 summarized all the data obtained.

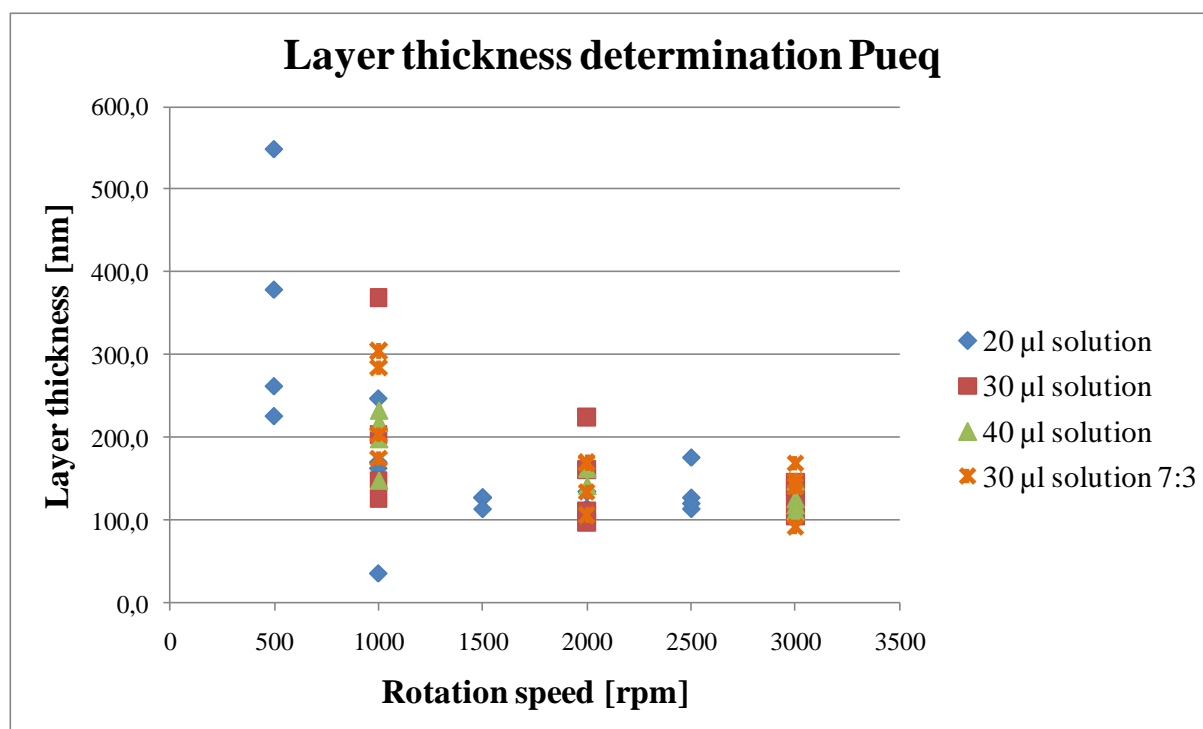


Figure 27: Results of the layer thickness determination for polyurethane

The different colors represent different amounts of polymer solution pipetted onto the electrodes before spin coating. All experiments showed the same behavior, namely that layer thickness decreases with increasing rotation speed, reaching saturation at around 1500 rpm. Furthermore increasing rotation speed means that the values are less scattered, leading to lower relative standard deviation at higher speeds. The experiments with 7:3 dilutions led to the most satisfying results with respect to relative standard deviation as well as layer thickness. Hence it was

decided that the best layer thickness could be achieved by using 1500 rpm with 30 μ l polymer solution at a 7:3 dilution.

Further experiments using these parameters led to layer thicknesses of about 254 ± 37 nm with a relative standard deviation of 15 %, which is acceptable.

4.3.4. Template removal from PUEq

In order to create cavities on the surface of the polymer film, template cells have to be removed. This was carried out according to the description in section [3.5.4], using different washing solutions on all polyurethanes tested, both catalyzed and non-catalyzed, and resulting from both imprinting methods, respectively.

None of the washing protocols proved suitable to remove the imprinted cells, as the optical microscope images in Figure 28 show.

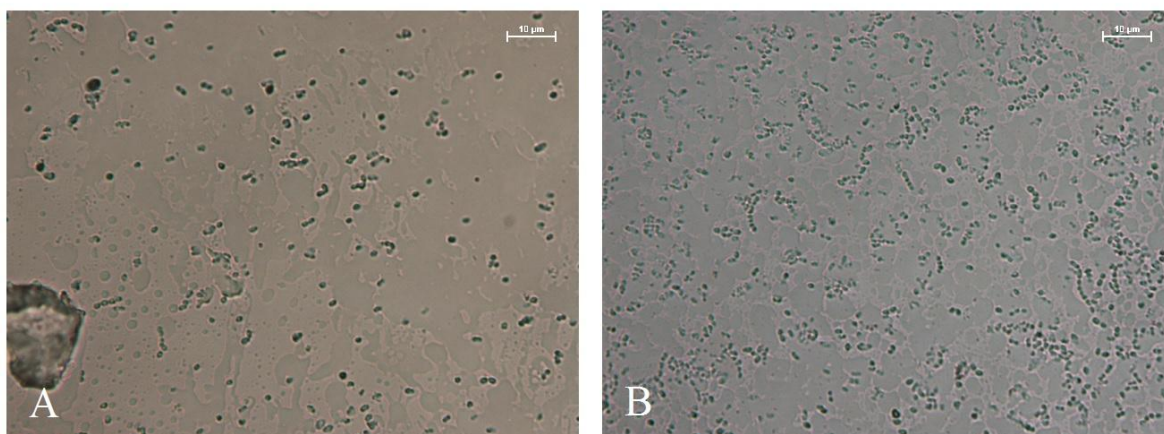


Figure 28: Comparison of A: unwashed imprinted cells and B: with all protocols washed imprinted cells in PUEq, non-catalyzed; 1000 times magnification

Image A shows the imprinted cells before all washing steps. Image B shows the cells after all washing steps. It can easily be seen that no cells have been removed. To ensure reliability of the images – the black dots could also be holes reflecting the light of the microscope in the right way – AFM images of the samples were recorded. Figure 29 shows an exemplary AFM image including the height profile of the cells measured.

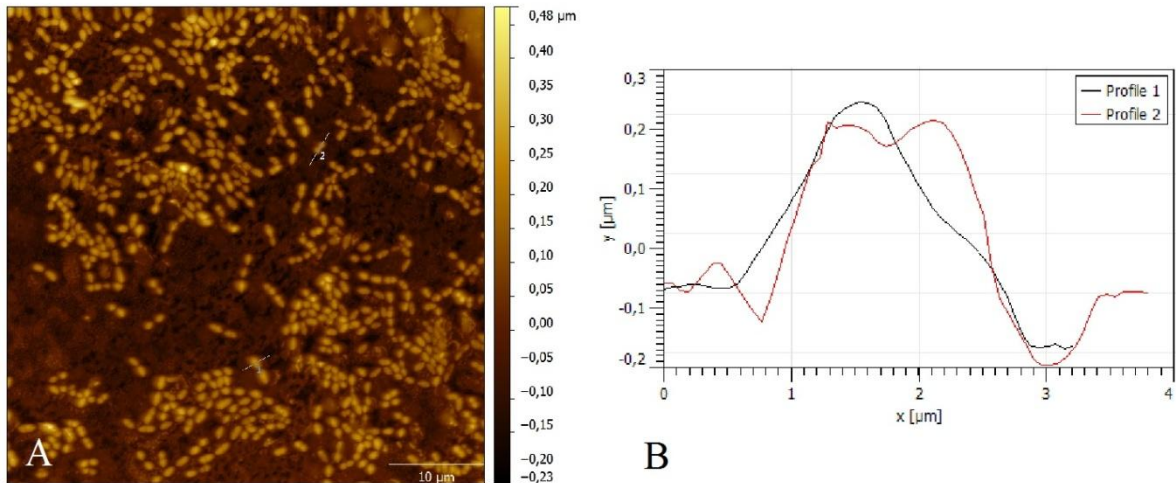


Figure 29: A: AFM picture of a washed glass slide; B: height profile extracted from the AFM picture

The profile shows that the measured cells protrude from the polymer surface by about 300 nm. Figure 29 A shows a large amount of immobilized cells, all extending from the polymer layer by about 0.3 μm . The cells are about 0.8 μm in diameter, which corresponds well to the theoretical size and shape of *S. epidermidis*: A single bacterium should be about 0.5 to 1.0 μm in diameter and spherical, according to Schleifer et al [26].

It can therefore be said that removing *S. epidermidis* was not successful and no cavities could be created by washing with the solutions mentioned in section [3.5.4]. A possible explanation for this behavior could be that a thin polymer layer crept on top of the cells while imprinting, protecting the cells against removal. A second explanation could be the inherent affinity of the bacterium towards plastics [27].

In order to create cavities on top of the polymer layer, further removing experiments featuring other washing solutions should be carried out. These experiments could not be realized in this thesis due to a lack of time.

The results of the removal experiments also indicate that the first QCM measurements using polyurethane and sedimentation imprint did work even though there have not been any cavities on the polymer surface, but only immobilized cells. A possible explanation for the QCM responses is that *S. epidermidis* tends to agglomerate naturally, especially in stress situations, as has been described previously (see section [2.5]). The cells in solution may adhere to the immobilized cells, building large but reversible agglomerates that lead to mass change and hence to a signal in the QCM measurement. In the scope of this thesis such behavior will be described as “agglomeration theory”.

4.3.5. QCM measurements

Even though it was not possible to remove the cells from the polymer, as described in section [4.3.4], QCMs using the ideal layer thickness and the sedimentation imprinting method were prepared and measured according to the description in section [3.5.5]. All sensors prepared showed similar response behavior and a success rate of 72 % working QCMs. One exemplary measurement is shown in Figure 30.

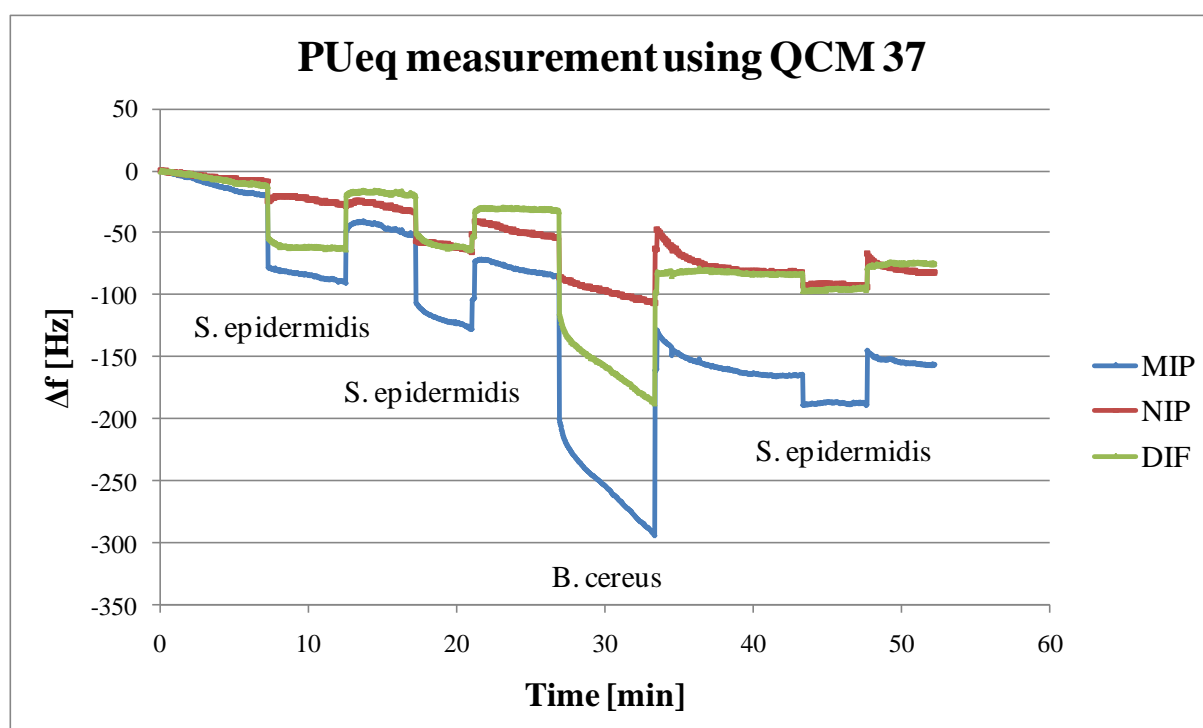


Figure 30: Exemplary QCM measurement using sedimentation imprinted PUeq

During these experiments *Bacillus cereus*, another rod shaped bacterium, was used as cross-reacting species in aqueous solution of approximately the same concentration as *S. epidermidis*. Evidently, the QCMs did respond with about 80 Hz to the analyte solution. However, the response to the cross-reacting compound was even stronger, about 180 Hz, questioning the selectivity of the sensors prepared. This result was repeated several times, leading to the conclusion that polyurethane may be suitable for creating a sensor for detecting different bacteria. However, polyurethane is not sufficiently selective for detecting *S. epidermidis*, as the PUeq-sensors also respond to *B. cereus* and *E. coli*.

According to the “agglomeration theory”, the recognition mechanism could be the agglomeration of the bacteria to immobilized individuals. Therefore inherent selectivity should be observable, as other organisms than *S. epidermidis* will most probably not agglomerate with the analyte due to natural competition. The lack of selectivity could be due to inherent affinities of the cross-reacting compounds to the polyurethane, or due to the possible coverage of the cells with a thin polymer layer as was mentioned before. Therefore the polymer system was changed to polymethacrylic acid, the second best suited polymer according to the screening experiments described in section [4.2].

4.4. Polymethacrylic acid

The composition of MIP based on polymethacrylic acid was not changed during this thesis due to lack of time. Therefore no polymer screening experiments were carried out with polymethacrylic acid.

4.4.1. Determining the layer heights of PA2THF

Following the details in section [3.6.1], layer thickness as a function of coating volume and spinning speed was assessed for polymethacrylic acid. The ideal layer thickness was again about 250 nm, due to the reasons discussed in section [4.3.3]. The results obtained of the experiments are summarized in Figure 31.

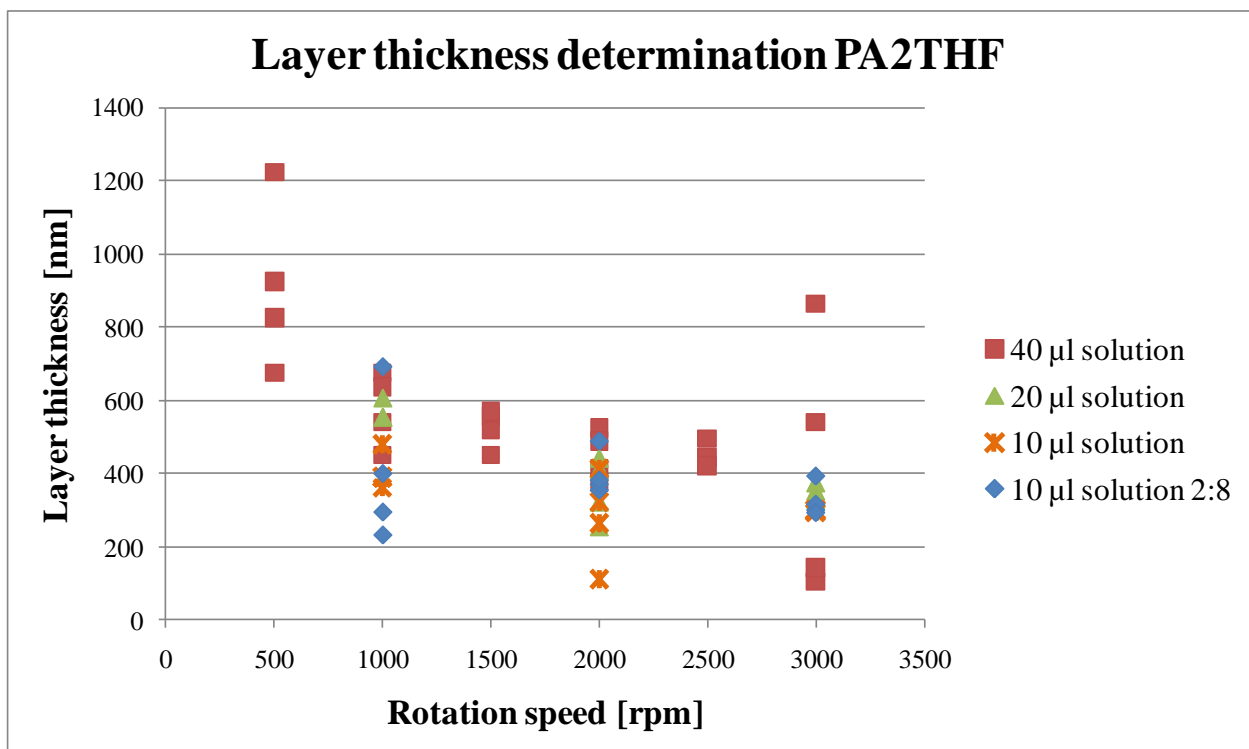


Figure 31: Results of layer thickness determination for polymethacrylic acid

All experiments showed similar behavior: Layer thickness decreases with increasing rotation speed, reaching saturation of decrease at around 1500 rpm, except when using 40 µl, which showed high variation at 3000 rpm. This effect may be due to the vast amount of polymer solution used, as the high volume may spread randomly at 3000 rpm, leading to high variation of layer thickness. The most satisfying results, however, could be achieved by using 10 µl of the

1:4 diluted solutions with a rotation speed of 3000 rpm, both regarding layer thickness and standard deviation.

Further experiments using 10 μl of the 1:4 diluted solutions at 3000 rpm lead to an average layer thickness of 221 ± 35 nm with a relative standard deviation of 34 %.

4.4.2. Template removal from PA2THF

As the polymer systems used show different properties and behavior it was assumed that the results achieved with polyurethane could not be transferred to polymethacrylic acid. Hence using PA2THF could make removal of cells and creation of cavities by washing possible. Therefore removal studies were carried out as described in section [3.6.2]. Once again the washing steps did not lead to any visible difference in the optical microscope, as the images before washing and after all washing steps except for NaOH / SDS in Figure 32 show.

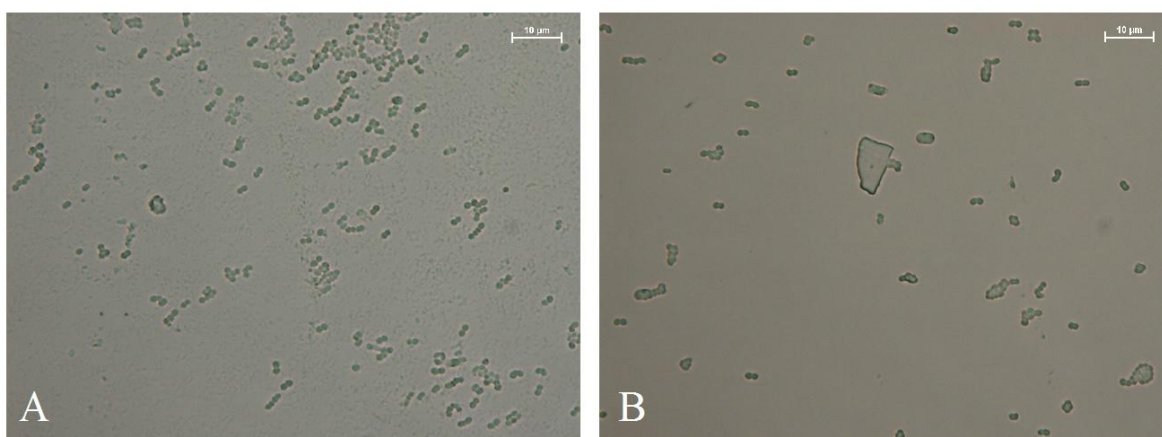


Figure 32: Comparison of A: unwashed imprinted cells and B: washed imprinted cells; 1000 times magnification

Both images were recorded with 1000 times magnification and show that cells remain in the polymer matrix. However, when washed with 0.1 % NaOH / SDS solution, the cells could be removed almost completely from the polymer surface, as shown in Figure 33.

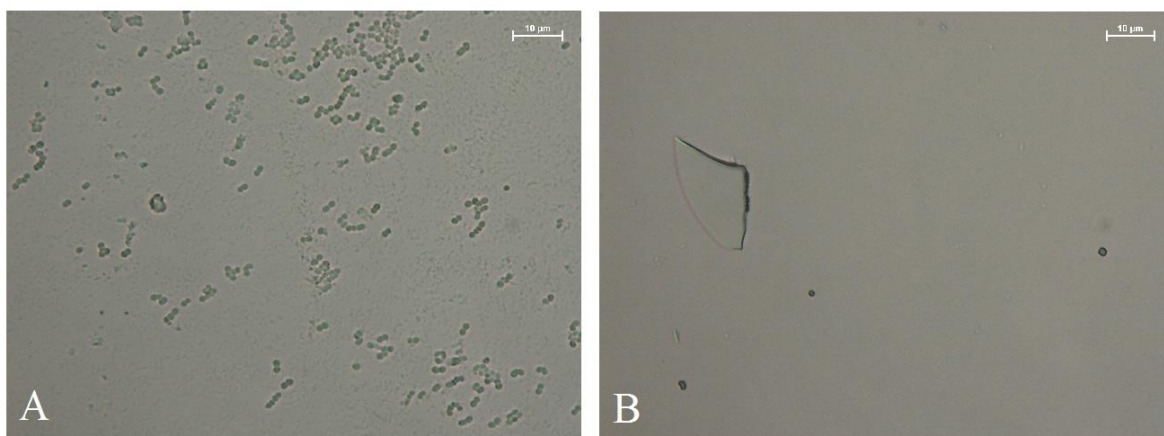


Figure 33: Comparison of A: unwashed imprinted cells and B: with NaOH / SDS washed imprinted cells; 1000 times magnification

Such complete removal of the cells first lead to the conclusion that cavities may have been created, but to prove this, AFM images had to be recorded. These, however, did not show any cavities, but proved that the washing solution had almost completely removed the polymer from the glass slides, as shown in Figure 34.

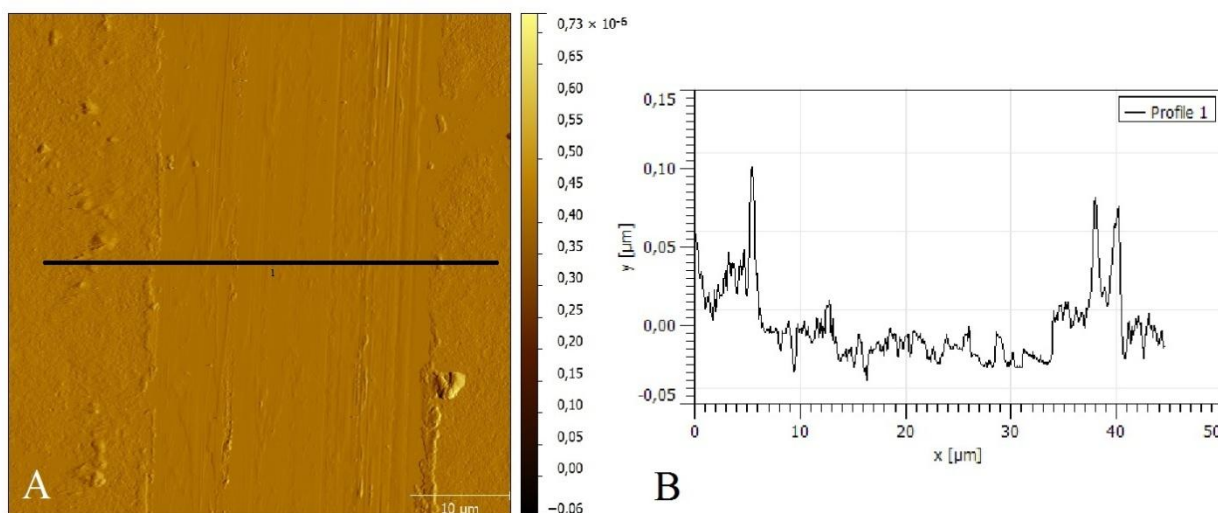


Figure 34: A: AFM image of a NaOH / SDS washed glass slide showing the razor blade cut; B: height profile of A

Figure 34 A shows the AFM image of a washed glass slide, containing no cavities, cut in the middle with a razor blade to determine the layer thickness of polymer on top of the slide. Figure 34 B shows the height profile over the whole width along the black line of picture A, showing that the layer thickness is only about 50 nm, which is way too low for any imprinting. This indicates that washing removed almost the whole polymer layer instead of only removing the

cells. This removal may be due to alkaline hydrolysis of the ester function in the cross linker, which destroys the polymer and its inter-chain connections. This results in increased water solubility of the shorter chains, which are then removed by water or SDS solution.

It was therefore concluded that the *S. epidermidis* cells could not be removed by the washing steps proposed. Anyway, the sensors may still work, as the “agglomeration theory” should also be applicable for other polymers than polyurethane.

4.4.3. APTES stamp imprint

As described in section [3.6.3], *S. epidermidis* cells have been immobilized onto glass slides in order to create stamps suitable for creating cavities on polymer surfaces. Figure 35 shows both, an optical microscope image as well as an AFM image of one of the stamps created.

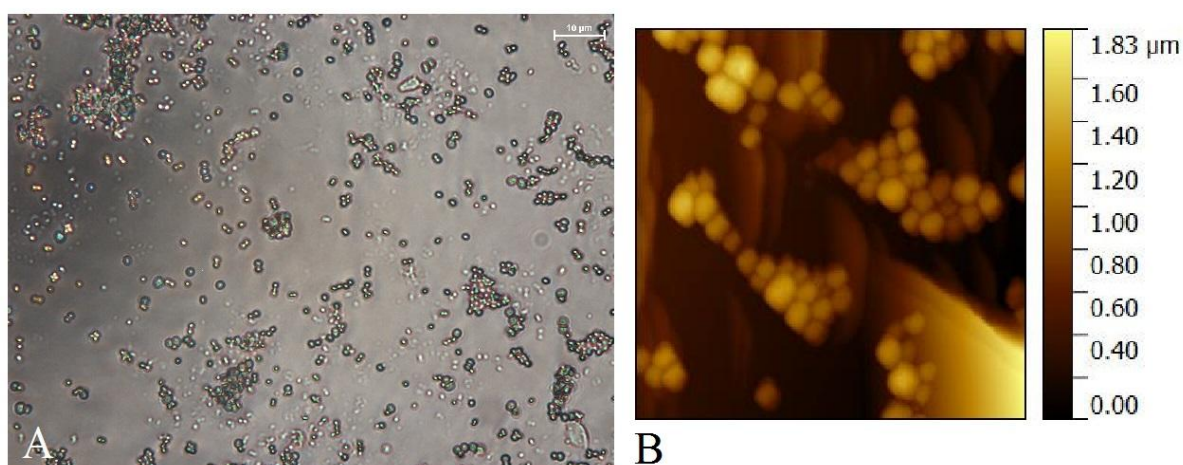


Figure 35: A: Optical microscope image of an APTES stamp with 1000 times magnification; B: AFM image of the same stamp

Figure 35 A shows the optical microscopy image with 1000 times magnification, Figure 35 B the AFM image (height profile) of the created stamp. It can easily be seen that a large number of cells have been immobilized. They are, beside surface irregularities, the highest points above the glass slides. It was therefore concluded that it should be possible to create cavities when pressing the stamps into freshly coated polymer.

This was, however, not possible with polymethacrylic acid, as the AFM images of an imprinted, polymer-coated glass slide and a QCM electrode shown in Figure 36 demonstrate.

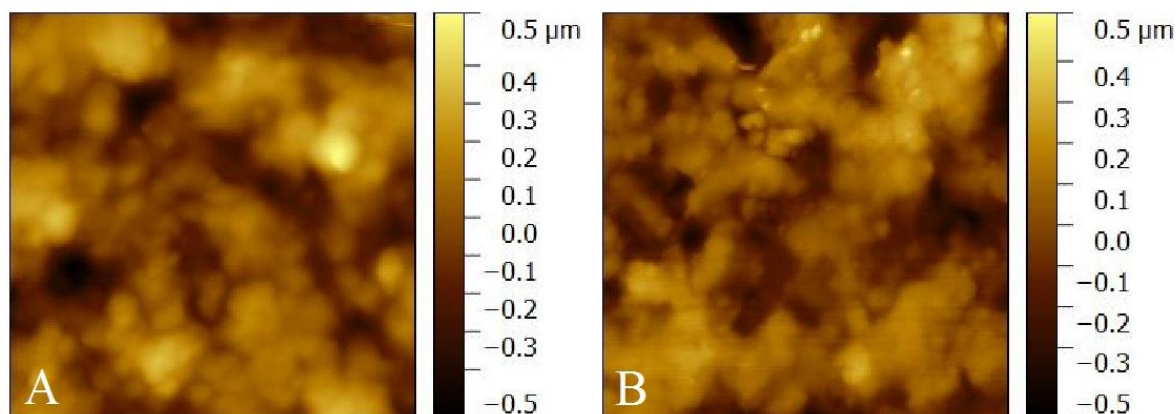


Figure 36: AFM images of A: an APTES stamp imprinted glass slide and B: a QCM electrode imprinted in the same way

Figure 36 A shows an imprinted glass slide; Figure 36 B an imprinted electrode on a QCM before measurement. It is clearly visible that neither cells nor cavities could be found on either sample, which proves that APTES stamp imprint was not successful in this first experiment. A total of more than 30 AFM images were recorded in order to find the cavities on top of imprinted substrates (glass slides and QCMs), but no measurement showed a single cavity.

One reason for the missing cavities could be the physical properties of the polymer. Polymethacrylic acid is softer than polyurethane [14] and may therefore be less suited for stamp imprinting. Another reason could be that by removing the stamp from the surface, cavities are torn apart. *S. epidermidis* shows inherent affinity to plastics [27] and may therefore bind strongly to the polymer, increasing the possibility of destroying the cavities by stamp removal.

Even though no cavities could be found, some QCMs produced with the APTES stamp imprint technique were assessed for their sensing properties as described in section [3.5.5] to ensure that the AFM pictures were not just very, very unlucky location picks but actually representing the average surface of the imprinted polymer layers. The measurements confirmed the AFM results in so far as no measurement led to satisfying results. One exemplary measurement is shown in Figure 37.

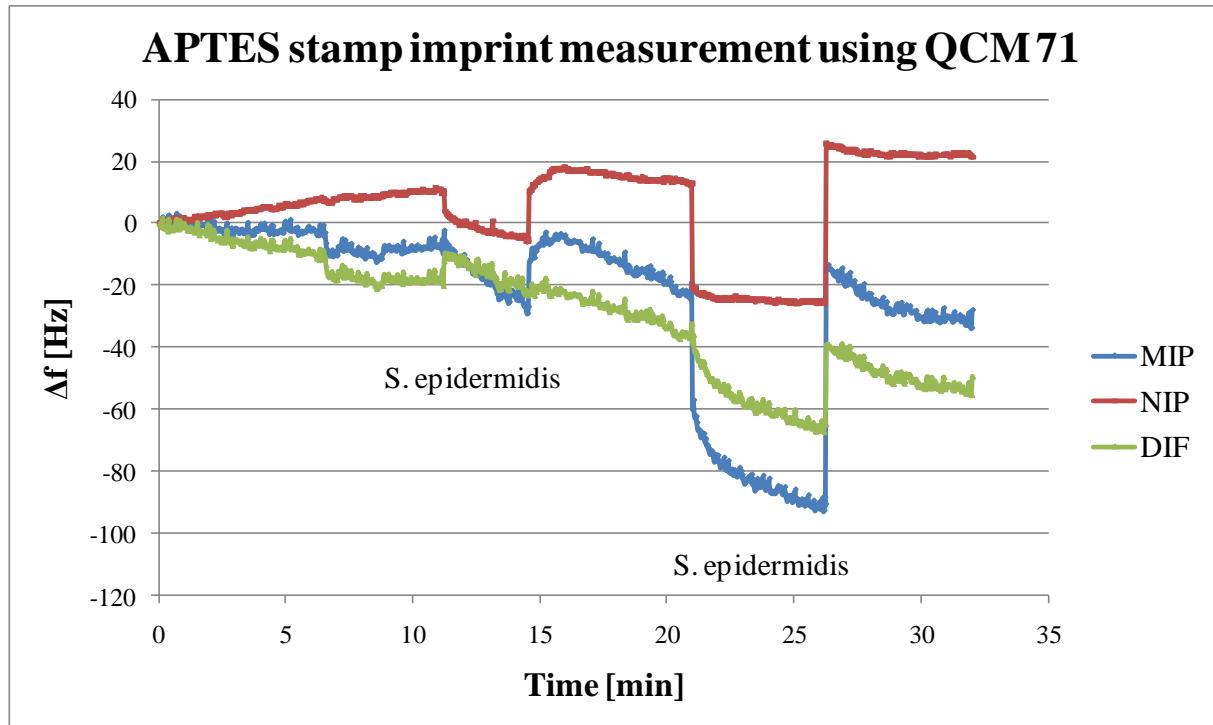


Figure 37: QCM measurement of an APTES stamp imprinted sensor

The measurement clearly shows that the responses to the analyte solutions are almost the same on both channels, the non-imprinted (red line) and the imprinted electrode (blue line). This leads to the conclusion that both, the MIP channel and the NIP channel, are the same, namely a non-imprinted polymer layer on top of the gold electrodes. The small difference may result from different polymer roughnesses, as a higher roughness offers more binding sides for the inherent affinity of *S. epidermidis*.

This result was repeated with several sensors, which is why APTES stamp imprint was discontinued.

4.4.4. QCM measurements

As the “agglomeration theory” should apply to any imprinted or immobilized *S. epidermidis* cells, QCM sensors for their detection using polymethacrylic acid were prepared and measured according to section [3.6.4]. The MIP channels for these experiments were sedimentation imprinted and the imprinted cells not removed. The QCMs showed both appreciable responses to the analyte solutions and selectivity against *B. cereus* and *E. coli*. One exemplary measurement is shown in Figure 38.

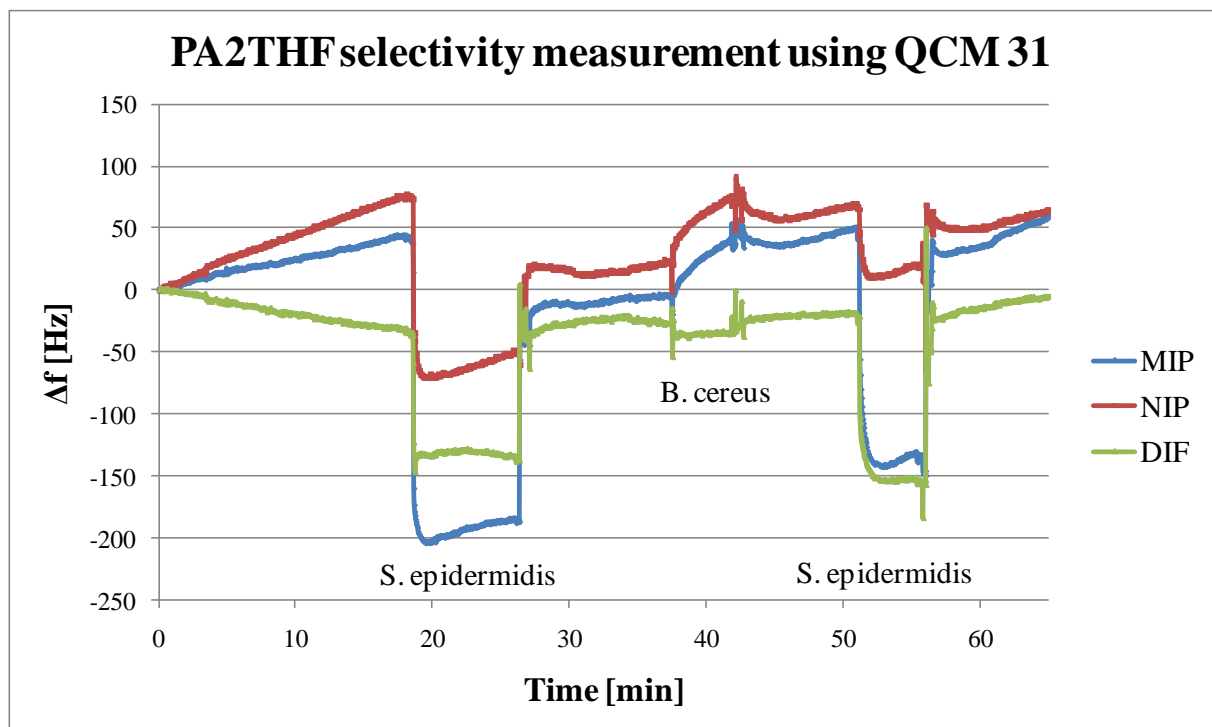


Figure 38: QCM measurement using sensor number 31

The concentrations of all measured solutions were approximately the same and about $2.5 \cdot 10^8$ cells / ml. As both signals for the *S. epidermidis* solution showed a 15 times higher response than the signal for the *B. cereus* solution, it was concluded that the sensors featuring polymethacrylic acid as imprinted polymer show a selectivity 15 times higher for the analyte than for the cross-reacting compound, as well as reasonable signals of about 150 Hz. The measurement above was repeatable with at least 18 other QCMs and the sensor production protocol used showed a success rate of about 75 %.

To further prove the “agglomeration theory”, AFM measurements of agglomeration QCMs were performed before and after measurements. Two AFM images, comparing a QCM before and after measurement, are shown in Figure 39.

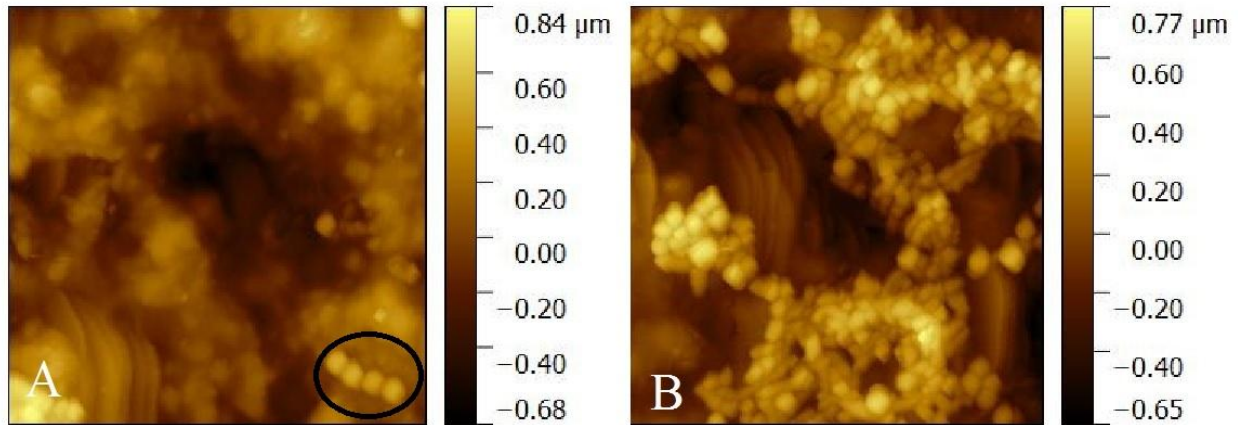


Figure 39: AFM pictures of a QCM A: before and B: after measurement

Picture A shows a QCM before measurements, only carrying a small chain of imprinted *S. epidermidis* cells (black circle). The circled dots were identified as *S. epidermidis* cells by their height and diameter, as well as the bright yellow dots in image B. These cells act as some kind of anchor for the other organisms in solution, enabling the adhesion of dissolved bacteria to the polymer surface, thus creating a signal on the sensor. Even though the signals created are reversible and the adhered cells are therefore removable, some of them remain on the polymer layer, most probably by strong interactions between cells and the polymer layer. Image B shows that AFM measurements found more cells on QCMs after measurements than on freshly prepared ones. This finding again supports the theory that *S. epidermidis* was mainly detected by agglomeration of the dissolved cells to the immobilized ones on the surface of the polymer layer, which led to a change in mass loading of the QCM and hence to the change in frequency observed in all measurements.

4.4.5. PA2THF Sensor characteristics

As it was possible to create QCM sensors for the detection of *S. epidermidis* according to the protocol in section [3.6.4], the sensor characteristics for these sensors were evaluated concerning the points described in section [2.1], which are response time, selectivity, repeatability or reversibility, ruggedness and detection limit. These parameters are summarized for one exemplary QCM, a sensor used for the stability study described in section [3.3] and 7 selectivity

and sensitivity measurements. The measurement determining the parameters in question is shown in Figure 40.

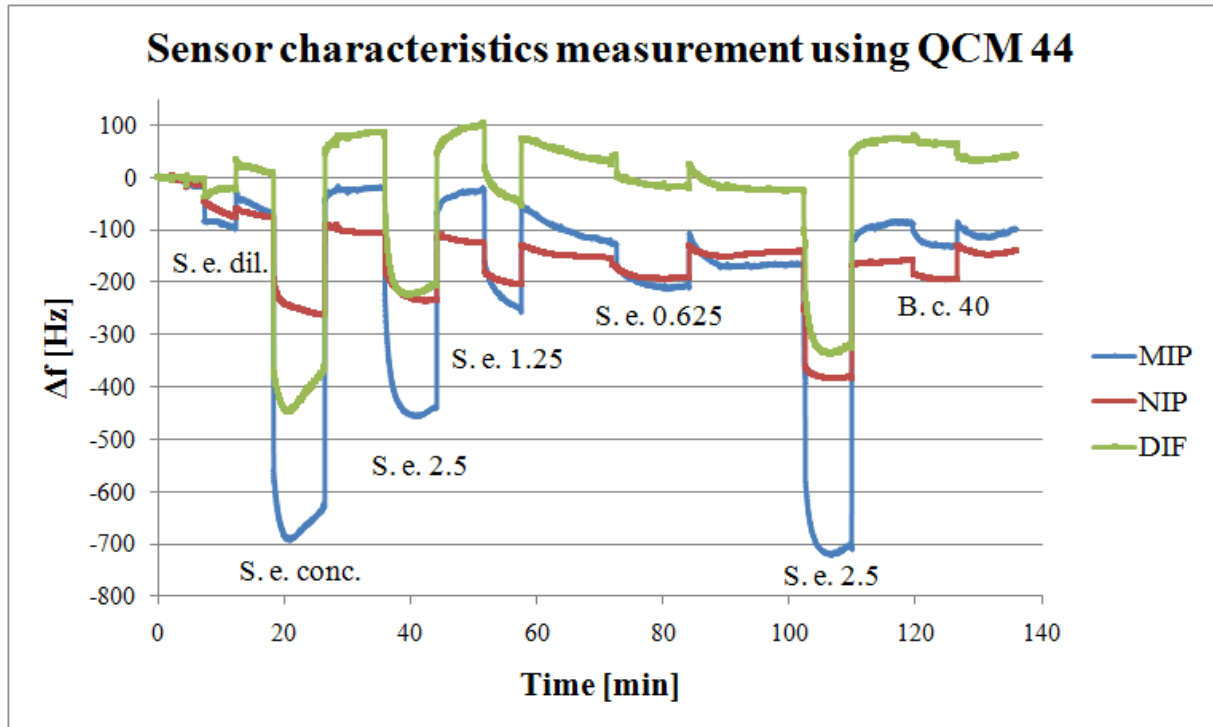


Figure 40: QCM measurement for the sensor characteristic using sensor number 44

The descriptions of the abbreviations used in the graph are explained in Table 7.

Symbol	Concentration [cells/ml]	Dilution	Signal [Hz]
S. e. conc.	random, high	-	398
S. e. dil.	random, low	-	18
S. e. 2.5	$2.5 \cdot 10^7$	1:1	300
S. e. 1.25	$1.25 \cdot 10^7$	1:2	115
S. e. 0.625	$0.625 \cdot 10^7$	1:4	48
B. c. 40	$4.0 \cdot 10^8$	1:1	12

Table 7: Symbols, concentrations, dilutions and signals for the QCM measurement in Figure 40

The signal is reversible. Furthermore it is also repeatable; because even after assessing several different concentrations, re-injecting previously assessed standard ha (S. e. 2.5) yielded almost the same response as before namely 290 Hz vs 310 Hz.

This QCM is also selective, as the response to a highly concentrated solution of *B. cereus* (see Table 7) was 70 times lower than the responses to lower concentrated *S. epidermidis* solutions. Similar results could be obtained for selectivity against *E. coli*, as presented in Figure 41.

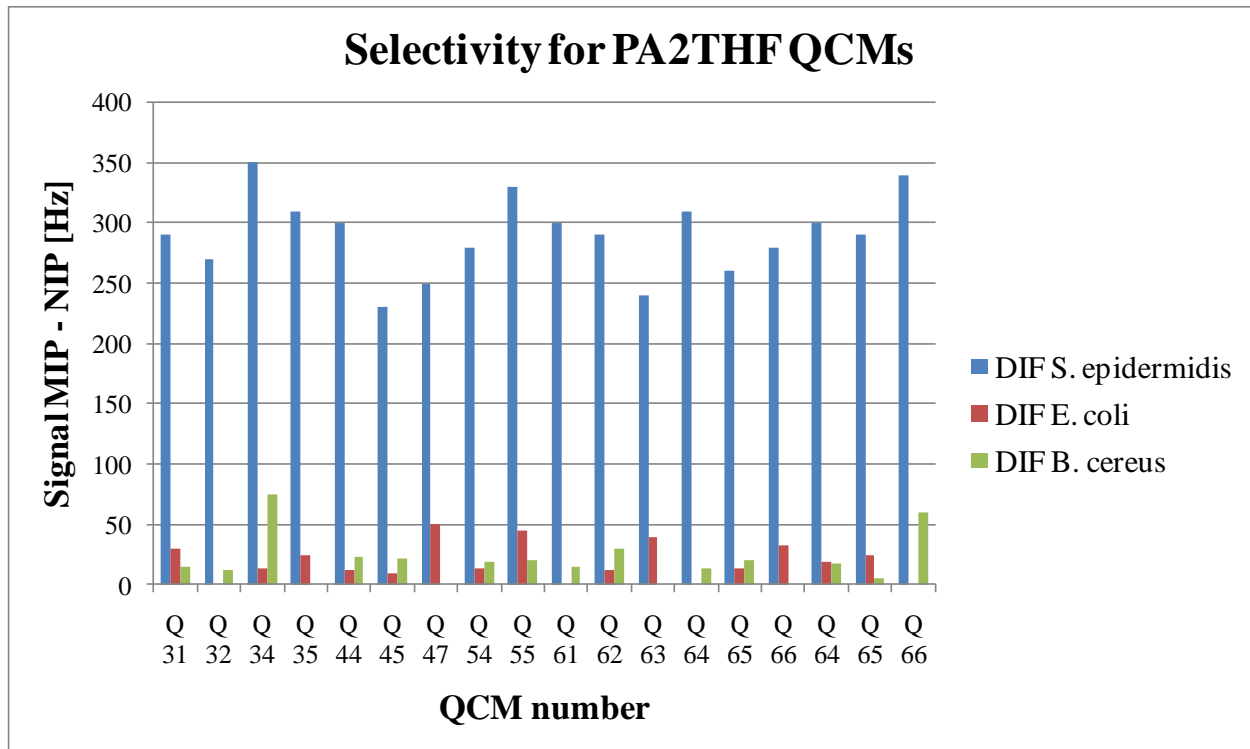


Figure 41: Selectivity results for *E. coli* and *B. cereus*.

Long-term stability of the sensor was tested according to section [4.1] plus a range of further experiments. QCM 44 showed 79 % signal intensity during the last measurement compared to the first one. It therefore lasted a period of about 2 months until it was broken to carry out AFM measurements. It can therefore be concluded that a QCM-based *S. epidermidis* sensor lasts at least 2 months, if stored in dry environment between measurements.

The response time can be obtained from the time the signal needs to stabilize from the point of injection onwards and is shown in Figure 42 for one of the injections of the measurement from above.

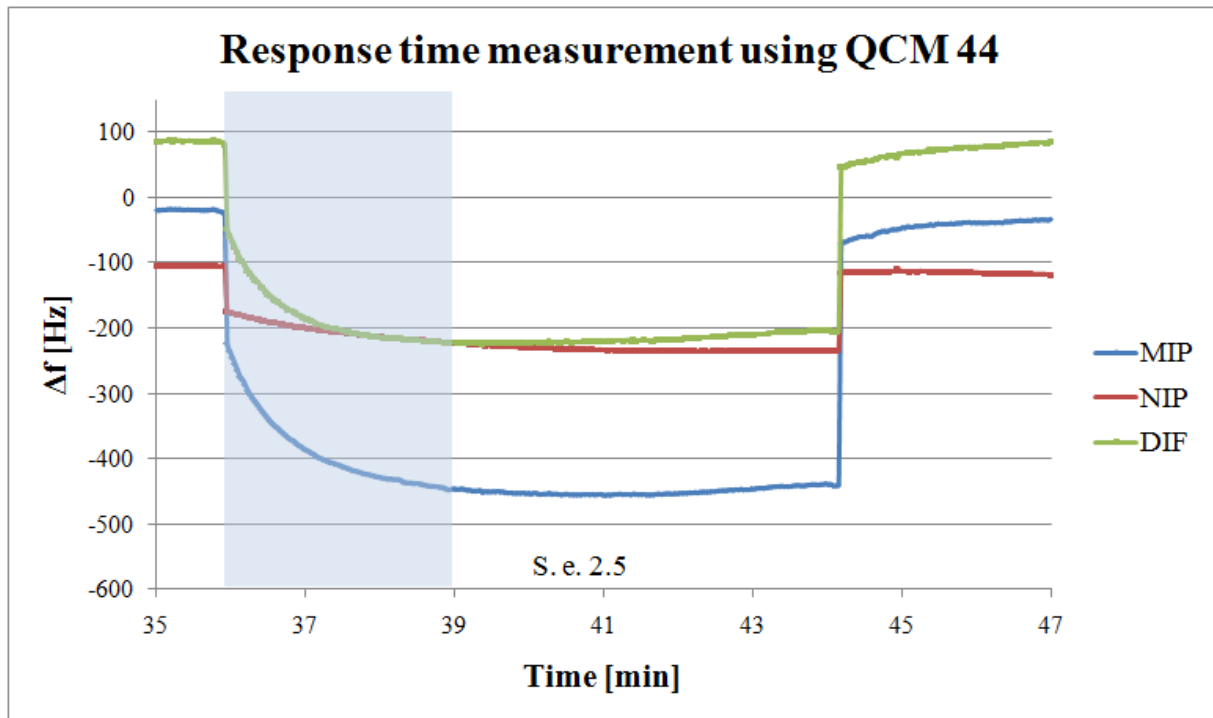


Figure 42: QCM measurement for the response time determination using sensor number 44

The area highlighted in pale blue is the time needed to stabilize the signal and was approximately the same for all QCMs measured. Therefore the response time of the *S. epidermidis* sensors is about 3 min \pm 20 sec. This time is, compared to the other methods introduced in section [2.9], reasonably fast and suited for detecting *S. epidermidis* in solution, especially as the cells try to coagulate and therefore may increase the signal in a flow through system.

The detection limit of the sensors was measured using a concentration range as given in Table 7 by plotting the concentration against the signal obtained and calculating the “point of zero signals” using simple linear regression. The plot obtained is shown in Figure 43.

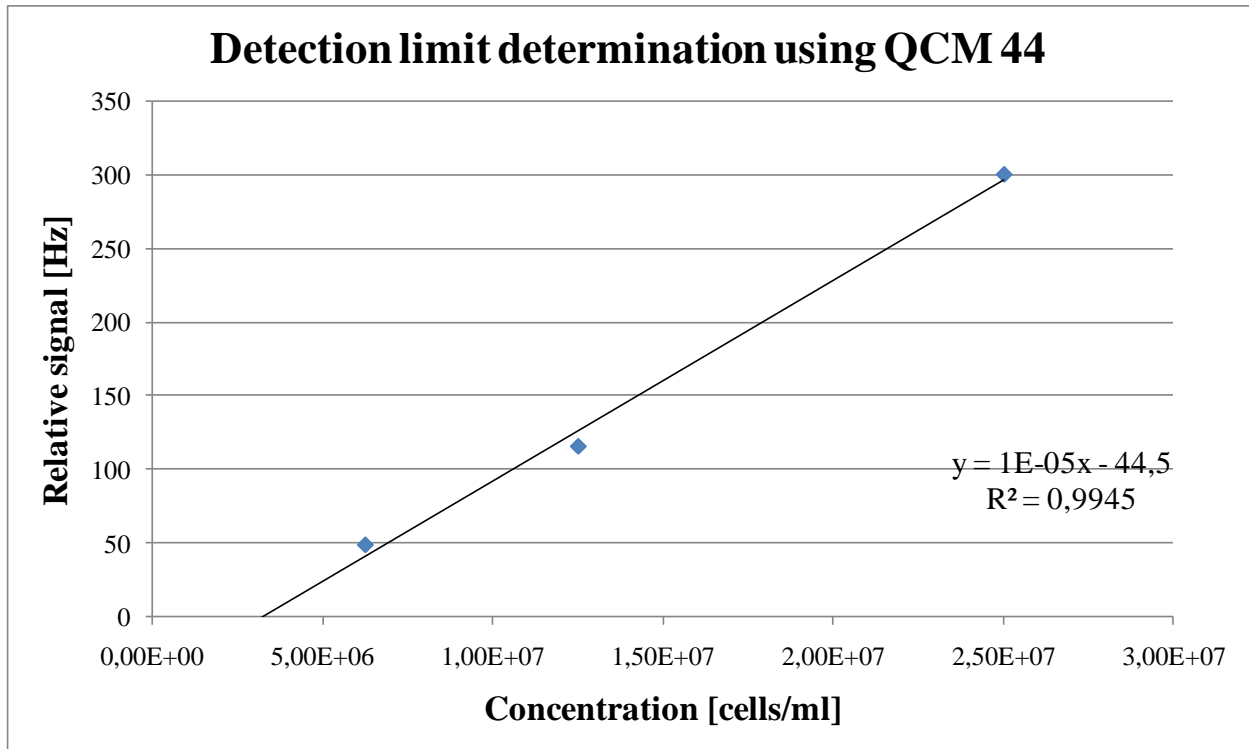


Figure 43: Linear regression plot of the detection limit determination

The calculated detection limit using the formula of the linear regression shown in the graph is approximately $4.5 \cdot 10^6$ cells / ml. The sensors are therefore able to detect concentrations of $5 \cdot 10^6$ cells / ml, which is 2 orders of magnitude lower than all concentrations used during this thesis, although it is quite a high concentration for water supplies. But as already mentioned, the tendency of the bacteria to agglomerate could enhance sensitivity, given the QCM enough time to “collect” individual cells in a flow - through system, i.e. preconcentrating them.

Finally it can be said that the sensors produced are able to fulfill all required properties, as they are sensitive, selective, sustainable and fast and the signals are repeatable as well as reversible. The stability or sustainability of the QCMs, however, needs further testing and the sensitivity is a question of need, as the limit of detection may still be unsuited for the detection of potentially infected water supplies.

5. CONCLUSION

5.1. Summarized conclusion

It could be shown that frozen bacteria solutions are stable for at least 7 days by both, microscopic observation and QCM measurements (see section [4.1]).

QCM polymer screening against blank gold electrodes showed that the polymer systems polyurethane and polymethacrylic acid are best suited for imprinting *S. epidermidis* (section [4.2])

Experiments carried out using polyurethane as a sensitive layer led to the conclusions that a polymer containing approximately the same amount of hydroxyl and isocyanate groups is best suited for imprinting when utilizing DABCO as a catalyst and drop imprinting as imprinting method (section [3.5.2]). Furthermore the ideal parameters for spin coating could be obtained (section [3.5.3]) and it has been shown that the imprinted cells could not be removed from the polymer in any way (section [4.3.4]).

This, however, did not have an influence on the quality of measurements (section [4.3.5]) and it was therefore concluded that the recognition mechanism is not of an analyte – cavity nature but more likely an agglomeration of *S epidermidis* to one another, which was named “agglomeration theory” (section [4.3.5]).

As the polyurethane QCMs did not show selectivity for the target analyte (section [4.3.5]), the polymer system used has been changed to polymethacrylic acid.

It was again possible to obtain ideal parameters for spin coating for polymethacrylic acid (section [4.4.1]), but not to remove imprinted cells from the polymer layer (section [4.4.2]).

A new stamp imprint method using APTES immobilized cells as stamps was tested with polymethacrylic acid, but neither AFM measurements nor QCM measurements showed any success with the APTES stamp imprinted substrates (section [4.4.3]).

Nevertheless, QCM sensors could be produced according to the recipe in section [3.6.4] that showed good selectivity and sensitivity (section [4.4.4]).

For the successful *S. epidermidis* sensors, using polymethacrylic acid and the agglomeration mechanism for detection, sensor characteristics could be obtained (section [4.4.5]) and evaluated.

Finally it can be said that it was possible to create a QCM sensor for the detection of *S. epidermidis* in aqueous solution with good sensor characteristics and a cheap way of production.

5.2. Prospects

Even though it was possible to create a fully functioning and selective QCM sensor for the detection of the targeted analyte, there is still potential to develop and need to improve the sensors obtained.

First of all a selectivity study should be carried out using a wider range of potential competitors like those present in water supplies. Furthermore measurements in tap water obtained from water supplies should be carried out, as all measurements in this work have been done in distilled water, and therefore potential matrix influences have not been taken into account.

In addition the APTES stamp imprint method could be tested on polyurethanes, because the different physical properties compared to polymethacrylic acid could enhance success of the stamp imprint. Hence it may be possible to create cavities in polyurethane using APTES stamps.

Another stability study concerning the effectivity of a QCM stored in agitated water for several days, weeks and finally months should also be carried out, as the stability of the sensors in a flow through environment has not been tested yet due to a lack of time.

Finally, if all parameters are optimized and tested for statistical security, the QCM sensors should be connected to sensors for other microorganisms and built into an electronic device capable of monitoring water supplies in the required way. This device should then be tested in an artificial test water supply and, if successful, compared to other detection methods.

It can ultimately be said that even though the production of a QCM sensor for the detection of *S. epidermidis* was successful, there is still potential for development and improvement, as is, was and will always be the case in scientific research and natural sciences.

6. UNITS AND ABBREVIATIONS

6.1. Abbreviations:

AFM	Atomic Force Microscopy
AIBN	2, 2-Azobis (2-methylpropionitrile)
<i>B. cereus</i> / <i>B. c.</i>	Bacillus cereus
BPA	Bisphenol A (4, 4'-(propane-2, 2-diyl) diphenole)
DABCO	1, 4-Diazabicyclo [2.2.2] octane
DHEBA	N, N'-(1,2-Dihydroxyethylene) bisacrylamide
DMF	Dimethylformamide
DNA	Deoxyribonucleic acid
DPDI	Diphenylmethane-4, 4'-diisocyanate
DUT	Device Under Test
<i>E. coli</i> / <i>E. c.</i>	Escherichia coli
EGDMA	Ethyleneglycoldimethacrylate
FWHM	Full Width at Half Maximum
hCG	Human chorionic gonadotropin
IUPAC	International Union of Pure and Applied Chemistry
MAA	Methacrylic acid
MDR	Multi Drug Resistant
MIP	Molecularly Imprinted Polymer
NaCl	Sodium Chloride
NIP	Non Imprinted Polymer
OCN	Isocyanate
OH	Hydroxyl
OsO ₄	Osmium tetroxide
PA	Polyacrylamide
PA2	Polymethacrylic acid
PCR	Polymerase Chain Reaction
PDMS	Polydimethylsiloxane
PET	Polyethylene terephthalate
PG	Phloroglucinol
PS	Polystyrene
PU	Polyurethane

PV Polyvinylpyrrolidone
QCM..... Quartz Crystal Microbalance
rpm Rounds Per Minute
S. epidermidis / *S. e.* Staphylococcus epidermidis
SDS..... Sodium dodecyl sulfate
STM..... Scanning Tunneling Microscope
THF Tetrahydrofuran
UV Ultra Violet

6.2. Units:

%..... Per Cent
°C..... Degree Celsius
A Ampere
dB Decibel
h..... Hour(s)
Hz Hertz
MHz..... Megahertz
min..... Minute(s)
mg Milligram
ng..... Nanogram
ml..... Milliliter
µl Microliter
sec..... Second(s)
V Volt

7. REGISTERS

7.1. Figure register

Figure 1: Schematic general sensor setup	9
Figure 2: Piezoelectric effect, scheme.....	10
Figure 3: Modes of vibration for an AT-cut quartz crystal; copyright by Jauch Quartz GmbH, 2007.....	11
Figure 4: Different angles of cutting a quartz crystal; copyright by Jauch Quartz GmbH, 2007.....	12
Figure 5: Gold electrodes on a QCM; Left: top-side electrode; Right: bottom-side electrode	14
Figure 6: Scheme of the bulk imprinting method	18
Figure 7: Scheme of the stamp imprinting method	19
Figure 8: Scheme of the sedimentation imprinting method	20
Figure 9: <i>S. epidermidis</i> , optical microscope image; 1000 times magnification	21
Figure 10: <i>S. epidermidis</i> , AFM image	21
Figure 11: Agilent 8712ET network analyzer.....	23
Figure 12: Principal setup of an optical microscope	24
Figure 13: Microscopic image (magnification 1000 times) of <i>S. epidermidis</i>	25
Figure 14: Scheme of an AFM.....	26
Figure 15: Measuring cell consisting of (from left to right):	31
Figure 16: Measuring system	32
Figure 17: 1000 times magnified aliquot pictures after A: 0 days; B: 1 day; C: 2days; D: 5 days; E: 7 days; F: 14 days	42
Figure 18: Stability study measurement for day 3	44
Figure 19: Ratios for MIP and the difference MIP - NIP against days; day 10 excluded.....	45
Figure 20: Affinity testing for polystyrene and polyurethane	46
Figure 21: Affinity testing for polyacrylate and polymethacrylic acid	47
Figure 22: First QCM measurement of <i>S. epidermidis</i> using polyurethane.....	49
Figure 23: Comparison of A: catalyzed PU and B: not catalyzed PU; 1000 times magnification	50
Figure 24: Comparison of A: sedimentation imprint and B: stamp imprint using catalyzed polyurethane; 1000 times magnification	51
Figure 25: Comparison of different polyurethane systems, 1000 times magnification. A: PUeq; B: PU5OH; C: PU10OH; D: PU25OH; E: PU50OH; F: PU10CN.....	53

Figure 26: Network analyzer measurement of QCM R49 Channel A	54
Figure 27: Results of the layer thickness determination for polyurethane.....	55
Figure 28: Comparison of A: unwashed imprinted cells and B: with all protocols washed imprinted cells in PUeq, non-catalyzed; 1000 times magnification.....	56
Figure 29: A: AFM picture of a washed glass slide; B: height profile extracted from the AFM picture	57
Figure 30: Exemplary QCM measurement using sedimentation imprinted PUeq.....	58
Figure 31: Results of layer thickness determination for polymethacrylic acid.....	60
Figure 32: Comparison of A: unwashed imprinted cells and B: washed imprinted cells; 1000 times magnification	61
Figure 33: Comparison of A: unwashed imprinted cells and B: with NaOH / SDS washed imprinted cells; 1000 times magnification	62
Figure 34: A: AFM image of a NaOH / SDS washed glass slide showing the razor blade cut; B: height profile of A.....	62
Figure 35: A: Optical microscope image of an APTES stamp with 1000 times magnification; B: AFM image of the same stamp.....	63
Figure 36: AFM images of A: an APTES stamp imprinted glass slide and B: a QCM electrode imprinted in the same way	64
Figure 37: QCM measurement of an APTES stamp imprinted sensor	65
Figure 38: QCM measurement using sensor number 31	66
Figure 39: AFM pictures of a QCM A: before and B: after measurement	67
Figure 40: QCM measurement for the sensor characteristic using sensor number 44.....	68
Figure 41: Selectivity results for <i>E. coli</i> and <i>B. cereus</i>	69
Figure 42: QCM measurement for the response time determination using sensor number 44.....	70
Figure 43: Linear regression plot of the detection limit determination.....	71

7.2. Table register

Table 1: Polymers used for polymer screening 35

Table 2: Different polyurethane compositions used 37

Table 3: Combinations of tested parameters 37

Table 4: Polyurethane compositions used for layer thickness determination 38

Table 5: Results of the stability study measurements 44

Table 6: Used polymers for polyurethane screening..... 52

Table 7: Symbols, concentrations, dilutions and signals for the
QCM measurement in Figure 40 68

7.3. Equation register

Equation 1: Sauerbrey equation 13

Equation 2: Kanazawa - Gordon equation 13

Equation 3: Modified Sauerbrey equation 15

Equation 4: Formula for the layer thickness calculation 15

Equation 5: Final formula for the layer thickness determination 16

Equation 6: FWHM formula 25

8. REFERENCES

1. **Engene JO.** "Five decades of terrorism in Europe: The TWEED dataset". *J Peace Res.* 2007;44(1):109-21.
2. "Threats to Food and Water Chain Infrastructure". In: Koukoulidou V, Ujevic M, Premstaller O, editors. *Threats to Food and Water Chain Infrastructure: Springer, Po Box 17, 3300 Aa Dordrecht, Netherlands; 2010.*
3. **Otto M.** "Staphylococcus epidermidis - the 'accidental' pathogen". *Nat Rev Microbiol.* 2009;7(8):555-67.
4. **Marx KA.** "Quartz crystal microbalance: A useful tool for studying thin polymer films and complex biomolecular systems at the solution-surface interface". *Biomacromolecules.* 2003;4(5):1099-120.
5. **Hulanicki A, Glab S, Ingman F.** "CHEMICAL SENSORS DEFINITIONS AND CLASSIFICATION". *Pure Appl Chem.* 1991;63(9):1247-50.
6. **Ghenadii K.** "Chemical Sensors Comprehensive Sensors Technologies". Momentum Press, LLC, New York. 2011;Volume 4. *Solid-State Sensors:500.*
7. **Curie JC, P.** "Développement par compression de l'électricité polaire dans les cristaux hémihédres à faces inclinées.". *Bulletin de la Société minérologique de France.* 1880;3(3).
8. **Kholkin A, Amdursky N, Bdikin I, Gazit E, Rosenman G.** "Strong Piezoelectricity in Bioinspired Peptide Nanotubes". *ACS Nano.* 2010;4(2):610-4.
9. **Janshoff A, Galla HJ, Steinem C.** "Piezoelectric mass-sensing devices as biosensors - An alternative to optical biosensors?". *Angew Chem-Int Edit.* 2000;39(22):4004-32.
10. "Quartz Crystal Theory". Jauch Quartz GmbH; 2007; Available from: www.jauch.de.
11. **Feigelson RS.** "50 years of progress in crystal growth - Preface". *J Cryst Growth.* 2004;264(4):XI-XVI.
12. **Sauerbrey G.** "VERWENDUNG VON SCHWINGQUARZEN ZUR WAGUNG DUNNER SCHICHTEN UND ZUR MIKROWAGUNG". *Zeitschrift Fur Physik.* 1959;155(2):206-22.
13. **Kanazawa KK, Gordon JG.** "THE OSCILLATION FREQUENCY OF A QUARTZ RESONATOR IN CONTACT WITH A LIQUID". *Anal Chim Acta.* 1985;175(SEP):99-105.

14. **Kim SC, Klempner D, Frisch KC, Frisch HL.** "POLYURETHANE INTERPENETRATING POLYMER NETWORKS .2. DENSITY AND GLASS-TRANSITION BEHAVIOR OF POLYURETHANE POLY(METHYL METHACRYLATE) AND POLYURETHANE-POLYSTYRENE IPNS". *Macromolecules*. 1976;9(2):263-6.
15. **Scientific Polymer Products I.** "Density of polymers". 2008 [cited 2016]; Available from: <http://scientificpolymer.com/density-of-polymers-by-density/>.
16. **Wulff G.** "MOLECULAR IMPRINTING IN CROSS-LINKED MATERIALS WITH THE AID OF MOLECULAR TEMPLATES - A WAY TOWARDS ARTIFICIAL ANTIBODIES". *Angew Chem-Int Edit Engl*. 1995;34(17):1812-32.
17. **Omidi F, Behbahani M, Samadi S, Sedighi A, Shahtaheri SJ.** "Coupling of Molecular Imprinted Polymer Nanoparticles by High Performance Liquid Chromatography as an Efficient Technique for Sensitive and Selective Trace Determination of 4-Chloro-2-Methylphenoxy Acetic Acid in Complex Matrices". *Iran J Public Health*. 2014;43(5):645-57.
18. **Bacsokay I, Takatsy A, Vegvari A, Elfving A, Ballagi-Pordany A, Kilar F, et al.** "Universal method for synthesis of artificial gel antibodies by the imprinting approach combined with a unique electrophoresis technique for detection of minute structural differences of proteins, viruses, and cells (bacteria). III: Gel antibodies against cells (bacteria)". *Electrophoresis*. 2006;27(23):4682-7.
19. **Lopez MM, Bertolini E, Olmos A, Caruso P, Gorris MT, Llop P, et al.** "Innovative tools for detection of plant pathogenic viruses and bacteria". *Int Microbiol*. 2003;6(4):233-43.
20. **Ramstrom O, Ansell RJ.** "Molecular imprinting technology: Challenges and prospects for the future". *Chirality*. 1998;10(3):195-209.
21. **Komiyama M, Takeuchi T, Mukawa T, Asanuma H.** "Fundamentals of Molecular Imprinting". *Molecular Imprinting: Wiley-VCH Verlag GmbH & Co. KGaA; 2004. p. 9-19.*
22. **Jenik M, Seifner A, Lieberzeit P, Dickert FL.** "Pollen-imprinted polyurethanes for QCM allergen sensors". *Anal Bioanal Chem*. 2009;394(2):523-8.
23. **Dickert FL, Lieberzeit P, Hayden O.** "Sensor strategies for microorganism detection - from physical principles to imprinting procedures". *Anal Bioanal Chem*. 2003;377(3):540-9.
24. **Foster WD.** "4 - The Discovery of the more Important Human Pathogenic Bacteria". *A History of Medical Bacteriology and Immunology: Butterworth-Heinemann; 1970. p. 64-91.*

25. **Zhang YQ, Ren SX, Li HL, Wang YX, Fu G, Yang J, et al.** "Genome-based analysis of virulence genes in a non-biofilm-forming *Staphylococcus epidermidis* strain (ATCC 12228)". *Mol Microbiol.* 2003;49(6):1577-93.
26. **Schleifer KH, Kloos WE.** "ISOLATION AND CHARACTERIZATION OF STAPHYLOCOCCI FROM HUMAN SKIN .1. AMENDED DESCRIPTIONS OF STAPHYLOCOCCUS-EPIDERMIDIS AND STAPHYLOCOCCUS-SAPROPHYTICUS AND DESCRIPTIONS OF 3 NEW SPECIES - STAPHYLOCOCCUS-COHNII, STAPHYLOCOCCUS-HAEMOLYTICUS, AND STAPHYLOCOCCUS-XYLOSUS". *Int J Syst Bacteriol.* 1975;25(1):50-61.
27. **Gottenbos B, van der Mei HC, Busscher HJ.** "Initial adhesion and surface growth of *Staphylococcus epidermidis* and *Pseudomonas aeruginosa* on biomedical polymers". *J Biomed Mater Res.* 2000;50(2):208-14.
28. **González G.** "Microwave transistor amplifiers: analysis and design: Prentice-Hall; 1984.
29. **Bardell D.** "The invention of the microscope". *BIOS (Ocean Grove).* 2004;75(2):78-84.
30. **Rayleigh.** "XXXI. Investigations in optics, with special reference to the spectroscope". *Philosophical Magazine Series 5.* 1879;8(49):261-74.
31. **Amos B, McConnell G, Wilson T.** "2.2 Confocal Microscopy A2 - Egelman, Edward H". *Comprehensive Biophysics.* Amsterdam: *Elsevier*; 2012. p. 3-23.
32. **Binnig G, Quate CF, Gerber C.** "Atomic Force Microscope". *Physical Review Letters.* 1986;56(9):930-3.
33. **Meyer G, Amer NM.** "NOVEL OPTICAL APPROACH TO ATOMIC FORCE MICROSCOPY". *Appl Phys Lett.* 1988;53(12):1045-7.
34. **Kilic A, Basustaoglu AC.** "Double triplex real-time PCR assay for simultaneous detection of *Staphylococcus aureus*, *Staphylococcus epidermidis*, *Staphylococcus hominis*, and *Staphylococcus haemolyticus* and determination of their methicillin resistance directly from positive blood culture bottles". *Res Microbiol.* 2011;162(10):1060-6.
35. **Ramirez-Arcos SM, Cameron C,** inventors; Canadian Blood Services, assignee. Method for detection of *Staphylococcus epidermidis* patent US 08673566. 2014 Mar 18 2014.
36. **Xiang K, Li YL, Ford W, Land W, Schaffer JD, Congdon R, et al.** "Automated analysis of food-borne pathogens using a novel microbial cell culture, sensing and classification system". *Analyst.* 2016;141(4):1472-82.

37. **Golabi M, Turner APF, Jager EWH.** "Tunable conjugated polymers for bacterial differentiation". *Sens Actuator B-Chem.* 2016;222:839-48.
38. **Baggiani C, Giovannoli C, Anfossi L, Passini C, Baravalle P, Giraudi G.** "A Connection between the Binding Properties of Imprinted and Nonimprinted Polymers: A Change of Perspective in Molecular Imprinting". *J Am Chem Soc.* 2012;134(3):1513-8.
39. **Yang XH, Yang WJ, Wang Q, Li HM, Wang KM, Yang L, et al.** "Atomic force microscopy investigation of the characteristic effects of silver ions on *Escherichia coli* and *Staphylococcus epidermidis*". *Talanta.* 2010;81(4-5):1508-12.
40. **Ji HS, McNiven S, Lee KH, Saito T, Ikebukuro K, Karube I.** "Increasing the sensitivity of piezoelectric odour sensors based on molecularly imprinted polymers". *Biosens Bioelectron.* 2000;15(7-8):403-9.
41. **Hu B, Zhu QK, Xu ZZ, Wu XB.** "High binding yields of viable cancer cells on amino silane functionalized surfaces". *Biomed Res-India.* 2015;26(3):452-5.
42. **Dastgheyb S, Hickok NJ, Otto M.** "Biofilm-Like Aggregation of *Staphylococcus epidermidis* in Synovial Fluid Reply". *J Infect Dis.* 2015;212(2):336-7.
43. **Schranzhofer L, Lieberzeit PA.** "Polymer-based receptors for silver and zinc oxide nanoparticles.". 2015.